Published in final edited form as:

Nature. 2016 April 14; 532(7598): 201–206. doi:10.1038/nature17644.

Modulation of tissue repair by regeneration enhancer elements

Junsu Kang[1], **Jianxin Hu**[2], **Ravi Karra**[3], **Amy L. Dickson**[1], **Valerie A. Tornini**[1], **Gregory Nachtrab**[1], **Matthew Gemberling**[1], **Joseph A. Goldman**[1], **Brian L. Black**[2], and **Kenneth D. Poss**[1]

[1]Department of Cell Biology, Duke University Medical Center, Durham, North Carolina 27710, USA

[2]Cardiovascular Research Institute, University of California, San Francisco, San Francisco, California 94143, USA

[3]Department of Medicine, Duke University Medical Center, Durham, North Carolina 27710, USA

Abstract

How tissue regeneration programs are triggered by injury has received limited research attention. Here, we investigated the existence of enhancer regulatory elements that engage in regenerating tissue. Transcriptome analyses revealed that *leptin b* (*lepb*) is sharply induced in regenerating hearts and fins of zebrafish. Epigenetic profiling identified a short DNA sequence element upstream and distal to *lepb* that acquires open chromatin marks during regeneration and enables injury-dependent expression from minimal promoters. This element could activate expression in injured neonatal mouse tissues and was divisible into tissue-specific modules sufficient for expression in regenerating zebrafish fins or hearts. Simple enhancer-effector transgenes employing *lepb*-linked sequences upstream of pro- or anti-regenerative factors controlled the efficacy of regeneration in zebrafish. Our findings provide evidence for tissue regeneration enhancer elements (TREEs) that trigger gene expression in injury sites and can be engineered to modulate the regenerative potential of vertebrate organs.

The capacity for complex tissue regeneration is unevenly distributed among vertebrate tissues and species. Salamanders and zebrafish possess remarkable potential to regenerate tissues like amputated appendages, resected heart muscle, and transected spinal cords[1,2]. Investigations of gene expression and function have generated molecular models for regeneration in multiple contexts, yet there is a deficiency in our understanding of the regulatory events that activate tissue regeneration programs[1–5].

Correspondence and requests for materials should be addressed to K.D.P. (kenneth.poss@duke.edu).

Supplementary Information is available in the online version of this paper.

Author Contributions J.K. and K.D.P. designed the experimental strategy, analysed data, and prepared the manuscript. J.K. generated transgenic zebrafish and performed regeneration experiments and analysis. J.H. and B.L.B. generated and analysed transgenic mice. R.K. generated and analysed sequencing datasets. A.L.D. performed surgeries and histology. V.A.T. generated and analysed mutant zebrafish. G.N., M.G. and J.A.G. contributed unpublished results and methodology. All authors commented on the manuscript.

The authors declare no competing financial interests. Readers are welcome to comment on the online version of the paper.

Recent genome-wide chromatin analyses suggest that gene regulatory elements comprise a substantial portion of genomic sequence. Of these elements, distal-acting regulatory sequences, or enhancers, represent the most abundant class[6,7]. Enhancers can direct expression of their target genes and have been predominantly examined as a means for stage- and tissue-specific regulation during embryonic development[8,9]. Studies have also implicated enhancers in disease and as targets during evolution[10–15]. Because of such findings, it is possible there may also exist enhancer elements that engage in response to tissue damage to regulate genetic programs for regeneration. The identification of such elements could potentially inspire solutions for manipulating regenerative events.

The *Leptin* ortholog *leptin b* is induced in regenerating zebrafish fin and cardiac tissues

To identify genes that are induced during tissue regeneration, we collected RNA from uninjured and regenerating tissues of adult zebrafish and sequenced transcriptomes. Our analyses identified 2,408 genes with significantly higher expression in tail fins at 4 days post amputation (dpa), and 859 genes with significantly higher expression in cardiac ventricles 7 days after induced genetic ablation of half of all cardiomyocytes (Extended Data Fig. 1a and Supplementary Tables 1 and 2). In total, 360 genes were induced 2-fold or greater in both tissues compared to uninjured tissues (Extended Data Fig. 1a). Among these genes, 69 were present at low levels in uninjured fins and induced sharply during regeneration (Supplementary Information). *leptin b (lepb)*, one of two zebrafish paralogs related to mammalian *Leptin*, a secreted regulator of energy homeostasis[16], had the highest relative change during fin regeneration of genes in this group (130-fold; Fig. 1c, Extended Data Fig. 2, and Supplementary Information). *lepb* transcripts were rare or undetectable in uninjured fins by semi-quantitative or quantitative RT-PCR (qPCR) or *in situ* hybridization (ISH), but induced in the regeneration blastema by 1 dpa (Extended Data Fig. 1b–d). Upon local injury of the cardiac ventricle by partial resection, *lepb* expression was induced in the endocardium, the endothelial lining of inner myofibers that has been implicated in regenerative events (Extended Data Fig. 1b, c, e)[17,18].

To capture the regulatory elements responsible for *lepb* induction, we replaced the first exon of *lepb* with an eGFP reporter transgene within a 150 kb BAC containing 105 kb of DNA sequence upstream of the start codon (Fig. 1d). Transgenic *lepb:eGFP* larvae had little or no detectable eGFP as viewed under a stereofluorescence microscope, and no fluorescence was detectable in fins or hearts throughout life (Fig. 1e and Extended Data Fig. 1h, i, l, m). Upon fin amputation, *lepb*:eGFP fluorescence was sharply induced in regenerating structures, where fluorescence localized to blastemal mesenchyme (Fig. 1e and Extended Data Fig. 1j, k). *lepb*:eGFP was also induced in wounds of resected ventricles, as well as in atrial tissue distant from the site of injury (Fig. 1g), a signature observed with other injury-induced markers[17,18]. While sparse *lepb*:eGFP could be detected in epicardial tissue at 1 day post resection (dpa; data not shown), cardiac *lepb*:eGFP fluorescence was predominantly endocardial by 3 dpa (Fig. 1g, h). Thus, sequences within a ~150 kb genomic region surrounding *lepb* direct regeneration-dependent expression in fin and cardiac tissues.

A sequence element upstream of *lepb* is sufficient for regeneration-activated expression

Enhancers are identifiable as areas of open chromatin, bound by transcription factors and occupied by histones possessing various modifications, such as acetylated lysine 27 of Histone H3 (H3K27ac)[19,20]. To define areas of open chromatin, we assayed genomic regions surrounding *lepb* for H3K27ac marks by ChIP-Seq in samples of uninjured and regenerating hearts. Two regions within the *lepb* BAC, located 7 kb and 3 kb upstream of the *lepb* start codon, were enriched with H3K27ac marks in regenerating, but not uninjured, samples (Fig. 2a and Extended Data Fig. 3a, b). To examine if either of these distal regions exhibited enhancer activity, we established several transgenic lines containing 2 kb, 6 kb, and 7 kb upstream sequences of *lepb* fused to an eGFP reporter gene (referred to hereafter as *P2:eGFP*, *P6:eGFP*, and *P7:eGFP*) (Fig. 2b and Extended Data Fig. 3c). Upon fin amputation, only *P7:eGFP* animals, with regulatory sequences encompassing the distal H3K27ac-rich area in the transgene, displayed strong blastemal expression that was comparable to *lepb:eGFP* BAC transgenic animals (Fig. 2c and Extended Data Fig. 3d; *P6:eGFP* fins showed expression below the amputation site). Similarly, whereas *P2:eGFP* and *P6:eGFP* animals occasionally displayed induced fluorescence in myocardium and epicardium after cardiac injury, only injured *P7:eGFP* hearts displayed strong endocardial fluorescence (Fig. 2c and Extended Data Fig. 3f). Thus, a short DNA element located 7 kb upstream of the *lepb* coding sequence is important for directing gene expression in regenerating adult tissues.

We next examined whether an isolated 1.3 kb sequence that corresponded to the H3K27ac-rich region could activate gene expression when fused to *P2*, which ostensibly includes the *lepb* promoter (Fig. 2b and Extended Data Fig. 3c). Although reporter eGFP fluorescence was not evident in uninjured adult fins or hearts of transgenic fish containing this *lepb*-linked distal element, fin amputation and ventricular resection activated eGFP fluorescence in blastemal and endocardial cells, respectively, in a similar manner to the *lepb* BAC sequences (Fig. 2c and Extended Data Fig. 3d–f). From a genome-wide H3K27ac survey, we also identified many 1–2 kb intergenic regions at other genomic loci that acquired H3K27ac marks during regeneration. We assessed sequence conservation and examined potential enhancer activity by transient transgenic reporter assays using several regions, some of which enabled expression from a minimal *lepb* promoter after injury (Extended Data Fig. 4a–d and Supplementary Information). To further validate the *lepb*-linked element, we examined its ability to influence the cell type-specific promoters *cmlc2* (cardiomyocytes) and *α-cry* (lens) in stable transgenic reporter lines. Robust, regeneration-dependent eGFP fluorescence was evident in fins and hearts of transgenic animals harboring either the *cmlc2* or *α-cry* promoters (Extended Data Figs. 5 and 9a, b, d, g). Thus, a small intergenic element we now refer to as *lepb-linked enhancer*, or *LEN*, can direct regeneration-activated gene expression from multiple promoters.

LEN-associated expression in injured neonatal mouse tissues

Analysis of regions upstream of *Leptin* genes in murine and human genomes revealed limited primary sequence conservation of *LEN* (Extended Data Fig. 4e). This sequence divergence likely reflects rapid evolution of enhancers, reported in previous studies[21,22]. To examine whether zebrafish *LEN* has activity in mammalian injury contexts, we fused it upstream of a construct containing a murine minimal *hsp68* promoter and a *lacZ* reporter gene. We generated two stable lines, one of which displayed vascular endothelial X-gal staining in uninjured neonatal hearts and paws (Extended Data Fig. 6b). A second line had a small number of X-gal-positive cells in uninjured neonatal tissues and was selected for injury studies (*LEN-hsp68::lacZ*) (Fig. 3a, b). Neonatal digit tips amputated at P2 phalanges do not regenerate lost structures effectively[23], whereas injured neonatal ventricles display a regenerative response[24]. Strikingly, amputated digit tips and damaged ventricles of all injured postnatal day 1 *LEN-hsp68::lacZ* neonates showed conspicuous X-gal staining in wounds 3 days following surgeries. A control transgenic line with an unrelated enhancer fragment also exhibited low basal expression in uninjured neonatal tissues, but unlike *LEN-hsp68::lacZ* animals, showed no detectable activation of the *lacZ* reporter upon injury to the digits or ventricle (Fig. 3a, b and Extended Data Fig. 6a). While tests of *LEN* activity using a panel of promoters and integration sites will be important, overall these results suggest that zebrafish *LEN* sequences can interact with mammalian transcriptional machinery to enable injury-induced expression in mice.

The *LEN* element is separable into tissue-specific regulatory modules

To identify minimal sequences responsible for the activity of *LEN*, we tested the ability of various fragments to direct regeneration-activated expression. We found that more distal *LEN* fragments composed of nucleotides 1–850, 450–1000, 450–850, or 660–850 could each drive eGFP expression from the *lepb* 2 kb promoter during fin regeneration (Fig. 4a, b and Extended Data Fig. 7). *LEN* fragments generated from the distal 1 kb portion also directed eGFP expression during fin regeneration when paired with the *cmlc2* promoter (Extended Data Fig. 5 and 9a, b). *LEN* fragments 1–850 and 450–1000 did not direct detectable eGFP expression during fin regeneration from the *α-cry* promoter in our experiments (Extended Data Fig. 5 and 9d–f), suggesting a repressive motif in *α-cry* upstream sequences. Intriguingly, none of these fragments directed endocardial expression after cardiac injury, although eGFP fluorescence was occasionally observed sparsely in epicardial cells or cardiomyocytes (Extended Data Fig. 8). Conversely, more proximal *LEN* fragments comprising nucleotides 830–1350 or 1000–1350 directed endocardial expression during heart regeneration, but did not activate eGFP fluorescence in regenerating fins (Fig. 4a, b and Extended Data Figs. 7 and 8). These proximal *LEN* fragments also could direct regeneration-associated expression in endocardial cells from *cmlc2* and *α-cry* promoters (Extended Data Fig. 9c, h). Thus, our analyses suggested the presence of two separate, tissue-specific enhancer modules (Fig. 4c).

We analyzed sequences of the minimal 190 nt (fin) and 316 nt (heart) elements, and identified distinct sets of predicted transcription factor binding motifs. *LEN(663–854)* contains predicted AP-1, Sox, Forkhead, and ETS binding sites, and we confirmed by

transgenic reporter assays that a predicted AP-1 binding site at *LEN(776–782)* is necessary to direct expression in regenerating fins (Extended Data Fig. 9i, j). *LEN(1034–1350)* contains predicted NFAT, GATA, Forkhead, and ETS binding sites, motifs associated with expression in endothelial cells[25,26] (Extended Data Fig. 9i). In total, our findings indicate a composite arrangement of regulatory elements with distinct tissue preferences within the *LEN* regeneration enhancer.

Engineered *LEN* element constructs can control regenerative capacity

Recent studies have described new enhancer-target gene pairings caused by chromosomal rearrangements that underlie genetic diseases like cancer and neurological disorders[10,12,15]. To examine a parallel idea for experimentally guiding tissue regeneration, we designed transgenic constructs positioning *LEN* and the minimal *lepb* promoter upstream of pro- or anti-regenerative factors. A possible outcome is that *LEN* would limit embryonic expression of potent developmental influences to permit maturation from the one-cell stage to adulthood, but also trigger and sustain expression of these influences upon tissue damage.

To create enhancer-effector transgenes, we took advantage of the dependency of fin regeneration on signaling by Fibroblast growth factors (Fgfs)[4,27]. We first positioned *LEN* upstream of a cDNA encoding a dominant-negative form of *fgfr1* (*dnfgfr1*) – a potent inhibitor of embryonic development[27,28] – and injected this construct into wild-type embryos. We established stable lines of zebrafish harboring either *P2:dnfgfr1* or *LENP2:dnfgfr1*, demonstrating that *dnfgfr1* expression was limited to developmentally insignificant levels. Adult *P2:dnfgfr1* fins displayed no detectable *dnfgfr1* induction after amputation and regenerated normally. By contrast, injury to *LENP2:dnfgfr1* animals induced strong expression of *dnfgfr1* (detectable by dnfgfr1-eGFP fusion protein fluorescence) that was restricted to the amputation plane. Moreover, these animals displayed conspicuous defects or outright failures in fin regeneration (Fig 5a, b). In some cases, fin rays failed to regenerate even by 30 dpa and maintained *dnfgfr1* expression in ray stumps, indicating persistent activation of *LEN* in the setting of regenerative failure (Fig 5c and Extended Data Fig. 10b).

We complemented these experiments with a gain-of-function approach, based on the discovery that mutations in the *fgf20a* ligand gene, *devoid of blastema* (*dob*), arrest fin regeneration[4]. We positioned *LEN* and the minimal *lepb* promoter upstream of a *fgf20a* cDNA and injected this construct into one-cell *dob* embryos. We generated stable lines of control *dob; P2:fgf20a* and *dob; LENP2:fgf20a* animals, indicating that these constructs restricted ectopic *fgf20a* expression during embryonic development. Upon amputation of adult tail fins, *dob; P2:fgf20a* animals induced no additional detectable *fgf20a* and displayed regenerative blocks comparable to *dob* animals (Fig. 5d, f, g). By contrast, *LENP2* sequences directed broad expression of *fgf20a* in mesenchymal cells upon fin amputation (Fig. 5d, f, g). Remarkably, blastemal cell proliferation was stimulated in amputated *dob; LENP2:fgf20a* fins, and these animals regenerated patterned structures that were often of normal length (Fig. 5e–g). In some cases, the lobed pattern of the tail fin was restored, and in no cases were there uncontrolled growth phenotypes (Fig. 5g).

Targeted stimulation of cardiomyocyte proliferation using the *LEN* element

Heart regeneration occurs through injury-induced stimulation of proliferation by pre-existing cardiomyocytes[29]. Recent evidence indicates that the secreted factor Neuregulin1 (Nrg1) is a cardiomyocyte mitogen during cardiac growth or repair in lower and higher vertebrates[30–32]. In zebrafish, *nrg1* is present at very low levels in the heart, and it is induced upon injury at levels that remain undetectable by standard ISH methodology[31]. Strong transgenic overexpression of *nrg1* in adult zebrafish cardiomyocytes activates overt cardiomyocyte proliferation and enlarges the ventricular wall[31]. To test whether *LEN* can influence heart regeneration, we created stable transgenic zebrafish lines with *P2:nrg1* or *LENP2:nrg1* constructs. Resection of the ventricular apex sharply increased *nrg1* transcripts in injured portions of *LENP2:nrg1*, but not control *P2:nrg1*, ventricles (Fig. 6a, b). *LEN*-induced *nrg1* expression was strongest in 7 dpa injury sites, slightly less prominent at 14 dpa, and scarcely detectable by 30 dpa, typically when a contiguous muscle wall has regenerated (Fig. 6a). To examine effects of targeted *nrg1* enhancement, we quantified cardiomyocyte proliferation indices in *LENP2:nrg1* and *P2:nrg1* ventricles at 14 dpa. *LENP2:nrg1* injury sites had a 52% increase in cardiomyocyte proliferation compared to *P2:nrg1* wounds, indicative of improved muscle regeneration (Fig. 6c, d). By 30 dpa, when *nrg1* levels approached baseline, regenerated ventricular walls appeared grossly normal (Fig. 6a). Thus, *LEN* can be designed to deliver mitogenic factors preferentially to areas of cardiac damage, boosting injury-induced cardiomyocyte proliferation.

Discussion

Here, we used a profiling approach to identify small regulatory elements that direct gene expression in regenerating tissue, which we now refer to as Tissue Regeneration Enhancer Elements (TREEs). Recently, a ~18 kb region of the murine *Bmp5* locus was reported to activate expression from minimal promoters in injury contexts[33], suggesting it may harbor a TREE analogous to the *LEN* element we describe here. We suspect that diverse classes of TREEs exist, including elements activated during development and re-activated by injury[34] or during regeneration, elements that activate expression preferentially during regeneration in multiple tissues, and regeneration-specific elements that are more tissue-restricted. The investigation of individual binding motifs within TREEs should identify upstream transcriptional regulators of regeneration, whereas genomic TREE locations can pinpoint novel downstream target genes.

Current methodologies to interrogate regenerative biology often have experimental disadvantages like multiple transgenes, ubiquitous promoters, irreversible expression, and/or stressful stimuli like estrogen analogs, tetracycline analogs, or heat shock[35]. By contrast, TREEs are single-transgene systems that can naturally induce and maintain target genes upon injury, and then naturally temper expression as regeneration concludes. Whereas *LEN* elements induce expression in fin mesenchyme and/or endocardium, we expect that future investigations will uncover a panel of regeneration-responsive TREEs representing additional distinct tissues. Thus, when combined with effectors, recombinases, or genome-editing enzymes, TREEs should facilitate targeted genetic manipulations that have been elusive to this point.

Multiple features of TREEs are appealing with respect to the design of potential regenerative therapies. Previous studies have implicated the manipulation of enhancer activity as a means to treat human genetic disease[12,36]. In this study, we report that pro- or anti-regenerative factors directed by TREEs are capable of blocking regenerative growth, promoting cell proliferation, or even rescuing genetic defects in regeneration. With a TREE-based system, factor delivery is spatiotemporally defined and could permit therapeutic cycles as injury recurs. Notably, although Nrg1 impacts heart regeneration, systemic neuregulin delivery has the potential for neurological or oncogenic effects[37,38]. Thus, enhancer-based targeting of Nrg1 to injury sites, as we model here in zebrafish, may represent a more effective regenerative medicine platform. We suggest that TREEs identified from natural regenerative contexts across vertebrate species can inform new strategies for precise factor delivery to injured human tissues.

Methods

Zebrafish maintenance and procedures

Wild-type or transgenic male and female zebrafish of the outbred Ekkwill (EK) strain were used for all experiments, with adults ranging in age from 3 to 12 months. Water temperature was maintained at 26°C for animals unless otherwise indicated. Fins were amputated to 50% of their original length using razor blades. As penetrance of the *dob* mutation was higher at 33°C than at 26°C, *dob* fish were maintained at 33°C after caudal fin amputation. To measure lengths of regenerates, lengths from the amputation plane to the distal tips of the 3rd and 4th fin rays of dorsal and ventral caudal fin lobes were determined using ZEN software. Because some *dob* animals regenerated portions of the 1st and 2nd fin rays of ventral lobes, regenerating caudal fin areas for Extended Data Fig. 10c were measured from the dorsal 3rd fin ray to the ventral 3rd fin ray and calculated using ZEN software. Partial ventricular resection surgeries were performed as described previously[39], in which ~20% of the cardiac ventricle was removed at the apex. To ablate cardiomyocytes, *cmlc2:CreER; bactin2:loxp-mCherry-STOP-loxp-DTA* (Z-CAT) fish were used[40]. Z-CAT zebrafish were incubated in vehicle (0.01% EtOH) or 10 μM tamoxifen for 12 hours. Work with zebrafish was performed in accordance with Duke University guidelines.

To generate *lepb:eGFP* BAC transgenic animals (full names, *Tg(lepb:eGFP)^{pd120} and Tg(lepb:eGFP)^{pd121}*), the *iTol2* cassette[41] was integrated into the BAC clone DKEY-21O22 using Red/ET recombineering technology (GeneBridges). Then, the first exon of the *lepb* gene in the BAC clone DKEY-21O22 was replaced with an *eGFP* cassette by Red/ET recombineering. 5′ and 3′ homology arms were amplified by PCR (Supplementary Information) and subcloned into the pCS2-eGFP plasmid. One nl of 50 ng/μl purified, recombined BAC was injected into one-cell stage zebrafish embryos along with one nl of 30 ng/μl synthetic *Tol2* mRNA[41]. To sort F_0 transgenic animals injected with *lepb:eGFP* constructs, fin folds were amputated at 3 or 4 dpf, and embryos displaying eGFP fluorescence near the injury site at 1 dpa were selected (Extended Data Fig. 1f). After raising F_0 zebrafish to adulthood, caudal fins were amputated and zebrafish displaying induced eGFP were selected for breeding (Extended Data Fig. 1g). Between 30–60 dpf, caudal fins of progeny from transgene-positive F_0 fish were amputated, and eGFP$^+$ transgenic animals

were isolated to identify stable lines. Two lines were identified that had indistinguishable expression features.

To define *LEN* activity, over 60 additional new transgenic lines were established in this study, listed in Supplementary Data 1. To generate transgenic animals, DNA sequences were amplified by PCR with indicated primers (Supplementary Data 3) and subcloned into a pCS2-eGFP-I-sceI vector, in which I-SceI restriction sites were flanked by a multiple cloning site. As promoters, 2 kb, 1.6 kb, and 0.7 kb upstream sequences of *lepb*, *cmlc2*[42], and *α-cry*[43] genes were used, respectively. These constructs were injected into one-cell-stage wild-type or *dob* embryos using standard meganuclease transgenesis techniques. 2 kb *lepb* upstream sequences could induce transgene expression after fin fold amputation at larval stages, but never after caudal fin amputation in adults. To isolate stable lines, larvae were examined for transgene expression near injury site in response to fin fold amputation (2 kb *lepb*), in cardiomyocytes (1.6 kb *cmlc2*), and in lens (0.7 kb *α-cry*).

To test additional TREEs, we subcloned putative enhancer regions of *il11a, plek, vcana*, and *cd248b* upstream of 800 bp of *lepb* upstream sequence (P0.8). To define TREE activity, these constructs were injected into one-cell-stage wild-type embryos, Fin folds were amputated at 4 dpf, and eGFP fluorescence near the amputation plane was examined at 5 dpf (1 dpa).

Generation and analysis of transgenic mice

Transgenic mice (CD-1 strain) were generated by oocyte microinjection as described previously[44]. *LEN-hsp68::lacZ* transgenic mice were generated by subcloning the zebrafish *LEN* enhancer sequence into the transgenic reporter plasmid *hsp68-lacZ*[45]. Ctrl-*hsp68::lacZ* transgenic mice harbor a transgene, *Prkaa2*[mMEF2(1+2)]-*hsp68-lacZ*, which contains a modified version of a 931-bp enhancer sequence from the mouse *Prkaa2* gene cloned into *hsp68-lacZ* (J. Hu and B. L. Black, unpublished observations). Partial apical resection injury in male and female neonatal mice at postnatal day 1 was performed similarly to previously described methods[46]. Hearts and paws were collected at postnatal day 4. All experiments with mice complied with federal and institutional guidelines and were reviewed and approved by the UCSF IACUC.

RNA isolation and quantitative PCR

RNA was isolated from dissected caudal fins and partially resected ventricles using Tri-Reagent (Sigma). cDNA was synthesized from 1 μg of total RNA using the Roche First Strand Synthesis Kit. Quantitative PCR was performed using the Roche LightCycler 480 and the Roche LightCycler 480 Probes Master. All samples were analyzed in biological triplicates and technical duplicates. Primer sequences are described in Supplementary Information, and probe numbers for *actb2, lepb*, and *nrg1* were 104, 156 and 76, respectively. *lepb* and *nrg1* transcript levels were normalized to *actb2* levels for all experiments.

RNA sequencing

Total RNA was prepared from two biological replicate pools of ablated Z-CAT ventricles and uninjured ventricles at 7 days post-ablation as per Gemberling et al.[31], or regenerating and uninjured caudal fins. Generation of mRNA libraries and sequencing were performed at the Duke Genome Sequencing Shared Resource using an Illumina HiSeq2000. Sequences were aligned to the zebrafish genome (Zv9) using TopHat[47]. Differentially regulated transcripts were identified using EdgeR and an FDR cut-off of 0.1[48]. Accession numbers for transcriptome datasets are GSE75894 and GSE76564.

ChIP sequencing

To identify candidate enhancer elements activated during heart regeneration, chromatin extracts were prepared from two biological replicate pools of 10 ablated Z-CAT ventricles and 10 uninjured ventricles. Chromatin was sonicated and immunoprecipitated with an antibody against H3K27ac (ActiveMotif) using the MAGnify ChIP system (Invitrogen). Sequencing libraries were prepared as per Bowman, et al.[49]. Sequencing was performed using an Illumina HiSeq2000, and 10–25 million 50 bp single end reads were obtained for each library. Sequences were aligned to the zebrafish genome (Zv9) using Bowtie2[50]. Differential peaks were identified using Model-based Analysis for ChiP-Seq (MACS)[51].

Histology and imaging

In situ hybridization on cryosections of 4% paraformaldehyde-fixed fins was performed as described previously[52]. To generate digoxigenin-labeled probes for *lepb* and *fgf20a*, we generated a fragment of *lepb* cDNA and a full length of *fgf20a* cDNA by PCR using primer sequences described in Supplementary Information. The *nrg1* probe was prepared as described previously[31]. Immunohistochemistry was performed as described previously[40]. Primary and secondary antibodies used in this study were: anti-Myosin heavy chain (mouse, F59, Developmental Studies Hybridoma Bank), anti-MEF2 (rabbit, sc-313, Santa Cruz Biotechnology), anti-PCNA (mouse, P8825, Sigma), anti-eGFP (rabbit, A11122, Life Technologies), anti-eGFP (chicken, GFP-1020, Aves Labs), anti-Raldh2 (rabbit, Abmart), anti-Ds-Red (rabbit, 632496, Clontech), anti-p63 (mouse, 4A4, Santa Cruz Biotechnology), Alexa Fluor 488 (mouse and rabbit; Life Technologies), Alexa Fluor 594 (mouse and rabbit; Life Technologies). For EdU incorporation experiments, zebrafish were injected intraperitoneally with 10 mM EdU (A10055, sigma), and caudal fins were collected at 1 hour post-treatment. EdU staining was performed as previously described[53]. The secondary antibody used for EdU staining was Alexa 488 azide (10–20 μM, Sigma). Whole-mount images were acquired using an M205FA stereofluorescence microscope (Leica) or Axio Zoom (Zeiss). Images of tissue sections (10 μm for hearts and 14 μm for fins) were acquired using an LSM 700 confocal microscope (Zeiss). X-gal staining to detect β-galactosidase activity and counterstaining with nuclear fast red were performed with murine tissue as described previously[44].

Data collection and statistics

Clutchmates were randomized into different treatment groups for each experiment. No animal or sample was excluded from the analysis unless the animal died during the

procedure. Sample sizes were chosen on the basis of previous publications and experiment types, and are indicated in each figure legend or methods. For expression patterns, at least five fish from each transgenic line were examined. At least 9 hearts of each group were pooled for RNA purification and subsequent RT-qPCR. Quantification of cardiomyocyte proliferation and calculation of statistical outcomes were assessed by a person blinded to the treatments. Sample sizes, statistical tests, and P values are indicated in the figures or the legends. One-way ANOVA tests were applied when normality and equal variance tests were passed. The Mann–Whitney rank sum test was applied in assays of cardiomyocyte proliferation.

Extended Data

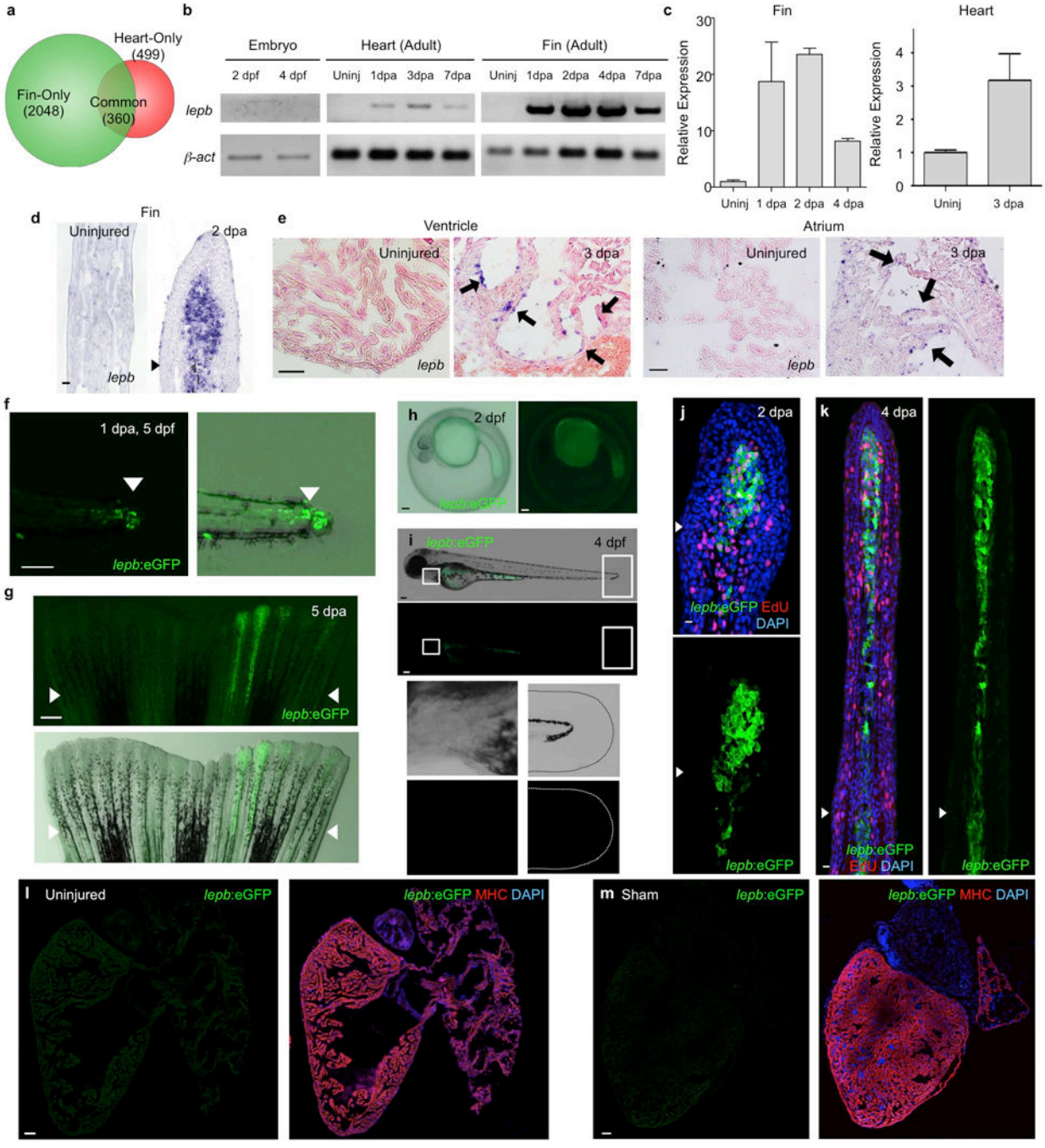

Extended Data Figure 1. *lepb* transcripts are sharply induced during fin and heart regeneration

a, Venn diagram displaying numbers of genes with significantly increased transcript levels during fin and heart regeneration. **b**, RT-PCR of samples from 2 days post-fertilization (dpf) and 4 dpf embryos, and uninjured and regenerating adult tissues. *lepb* was not detected during embryogenesis and in uninjured tissues, but induced during regeneration. *β-act2* is used as loading control. Uninj, Uninjured. **c**, (Left) Relative expression of *lepb* in uninjured,

1, 2, and 4 dpa fin regenerates. *lepb* transcript levels are increased at 1 and 2 dpa. (Right) Relative expression of *lepb* in uninjured or 3 dpa cardiac ventricles, assessed by qPCR. **d, e**, Endogenous *lepb* expression assessed by *in situ* hybridization in sections of fins (**d**) and cardiac ventricle and atrium (**e**). Arrowhead, amputation plane. Arrows, endocardial *lepb* expression. Left: uninjured tissues, Right: regenerating tissues. dpa: days post-amputation. **f, g**, F_0 animals, injected with the transgenic *lepb:eGFP* BAC reporter construct at the one-cell stage, induced eGFP after larval fin fold amputation (**f**) and during adult fin regeneration (**g**). Note that *lepb*:eGFP is mosaically expressed. Arrowheads, amputation planes. **h, i**, Expression pattern of *lepb:eGFP* stable transgenic animals. *lepb*:eGFP was not detected in fin and heart during embryogenesis (**h**, 2 dpf; **i**, 4 dpf). Below '**i**' are enlargements of the boxed areas, which show heart (left) and fin fold (right). Dotted line, outline of fin fold. The yolk is autofluorescent. **j, k**, Section images of *lepb:eGFP* caudal fin regenerates at 2 dpa (**j**) and 4 dpa (**k**). The majority of *lepb*:eGFP-positive cells are mesenchymal cells, overlapping partially with cells that incorporate EdU (collected 60 minutes after injection; red). **l, m** Lack of detectable expression of *lepb*:eGFP in hearts of uninjured **(l)** or sham-operated **(m)** *lepb:eGFP* animals. n = 8 and 5 for uninjured and sham-operated hearts, respectively. Arrowheads, amputation planes. Scale bars: **d**, **f**, **h–k**, 10 μm; **e, l, m**, 50 μm; **g**, 500 μm.

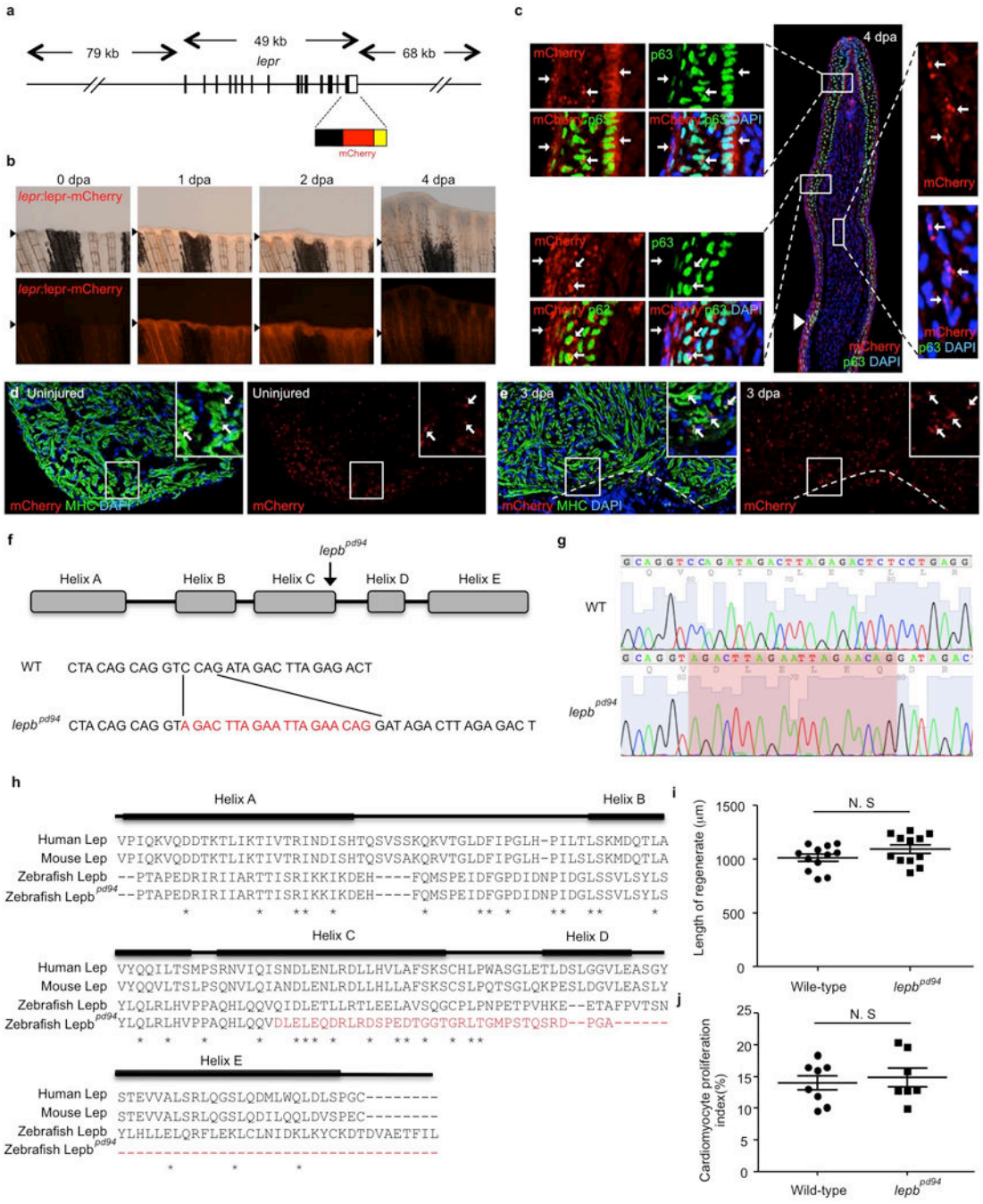

Extended Data Figure 2. Leptin signaling during fin and heart regeneration

a–e, Expression pattern of *lepr:lepr-mCherry* BAC reporter line. **a**, Schematic of the *lepr:lepr-mCherry* BAC transgenic construct. mCherry is fused at the C-terminus of Lepr. **b**, mCherry fluorescence in the *lepr:lepr-mCherry* BAC reporter strain is induced during fin regeneration. n = 5; all animals displayed a similar expression pattern. **c**, Section images of 4 dpa *lepr:lepr-mCherry* caudal fin regenerates. The majority of Lepr-mCherry^{+} cells are epidermal cells, overlapping partially with p63^{+} basal and suprabasal cells (left). In addition, some putative vascular cells in the intraray region have Lepr-mCherry signals (right). **d, e**,

Confocal images of sections through uninjured **(d)** and regenerating **(e)** *lepr:lepr-mCherry* hearts. Lepr-mCherry fluorescence co-localizes with MHC^{+} cardiomyocytes in uninjured and 3 dpa hearts (arrows). Note that these expression patterns are similar to Leptin receptor expression in mice (See Supplementary Information). n = 7 and 6 for uninjured and 3 dpa hearts, respectively. **f–j**, Analysis of fin and heart regeneration in *lepb*^{pd94} mutants. **f**, A schematic representation of Lepb, showing the effects of the *pd94* mutation. Lepb is composed of 5 alpha-helix domains. *lepb*^{pd94} has a 19 bp insertion and a 3 bp deletion at the 3rd α-helix (Helix C). **g**, Sequencing of wild-type and *lepb*^{pd94} alleles revealed an indel (Red highlight). **h**, A comparison of the amino acid sequences of *Leptin* genes in of human, mice, and zebrafish. The predicted amino acid sequence of the *lepb*^{pd94} gene product is shown at the bottom, with the predicted truncation sites indicated in red. The predicted *lepb*^{pd94}protein product lacks the majority of C-terminal amino acids. *Identical amino acid residue between three species. **i**, Quantification of regenerated fin lengths from *lepb*^{pd94} and wild type siblings at 4 dpa. n = 12 each of *lepb*^{pd94} and wild-type. **j**, Quantification of cardiomyocyte proliferation at 7 dpa. n = 7 (*lepb*^{pd94}) and 8 (wild-type). Data are represented as mean ± SEM. N.S, Not significant.

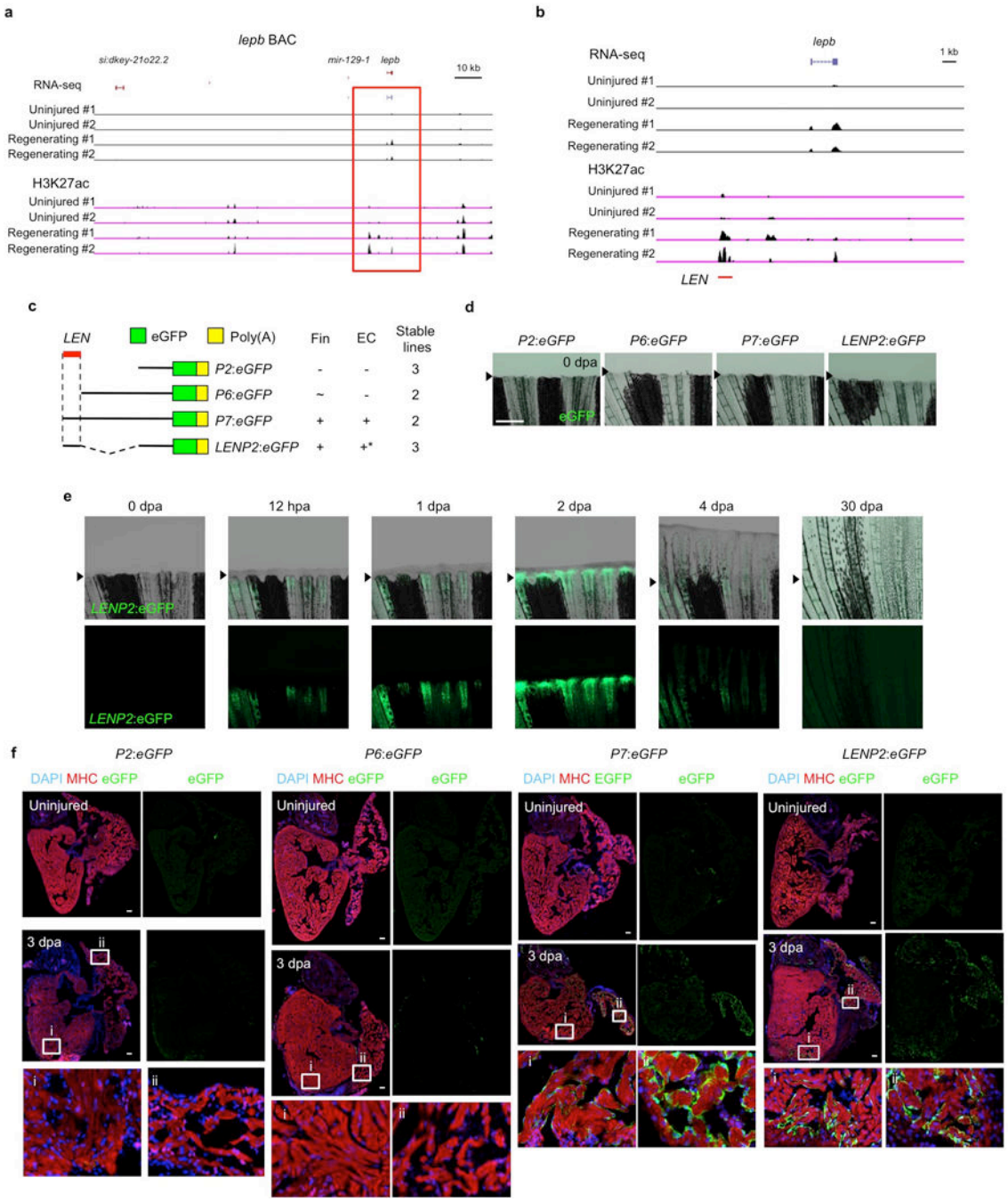

Extended Data Figure 3. Identification of *LEN* and tests of regulatory sequences near *lepb*

a, Schematic depicting the genomic region surrounding *lepb* (corresponding to the *lepb* BAC used in this study) with the profiles of RNA-sequencing and H3K27ac marks from uninjured and regenerating heart tissues. **b**, Enlargement of the boxed area in **a**. *lepb* is the only upregulated gene in this genomic region during regeneration. H3K27ac-enriched peaks in regenerating samples are present in a ~1 kb region (red bar) that is ~7 kb upstream of the start codon. **c**, Schematic representation of transgenes to examine regulatory sequence activity. Fin and endocardial expression during regeneration and the number of stable lines

are indicated. *One *LENP2:eGFP* line showed occasional, weak endocardial eGFP expression in uninjured hearts, whereas eGFP signal in this line was broad and strong during regeneration. EC, endocardial cells. **d**, Images of representative 0 dpa fins from lines indicated in (**c**). eGFP fluorescence is not detectable in fins at 0 dpa or in uninjured fins, but is induced in regenerating ray blastemas in *P7:eGFP* and *LENP2:eGFP* lines. *P6:eGFP* regenerates displayed weak eGFP expression below the amputation plane during regeneration, with very weak or undetectable expression in regenerating portions (see Fig. 2c). **e**, *LENP2*:eGFP expression pattern during fin regeneration. eGFP is detectable as early as 12 hpa, but is undetectable at 30 dpa. n = 5; all animals displayed a similar expression pattern. Arrowheads, amputation planes. **f**, Section images of representative uninjured and regenerating hearts from *P2:eGFP*, *P6:eGFP*, *P7:eGFP*, and *LENP2:eGFP* animals. eGFP fluorescence is rarely detectable in uninjured *P2:eGFP, P6:eGFP, P7:eGFP*, or *LENP2:eGFP* hearts, except in one line of *LENP2:eGFP* (mentioned above). Upon injury, *P2* drove weak, occasional expression in cardiomyocytes and epicardium but not in endocardium, whereas *P7* and *LEN* drove endocardial eGFP expression in ventricle and atrium. i, ii, enlargements of boxes areas in regenerating ventricle and atrium, respectively. Scale bars: **d, e**, 500 μm; **f**, 50 μm.

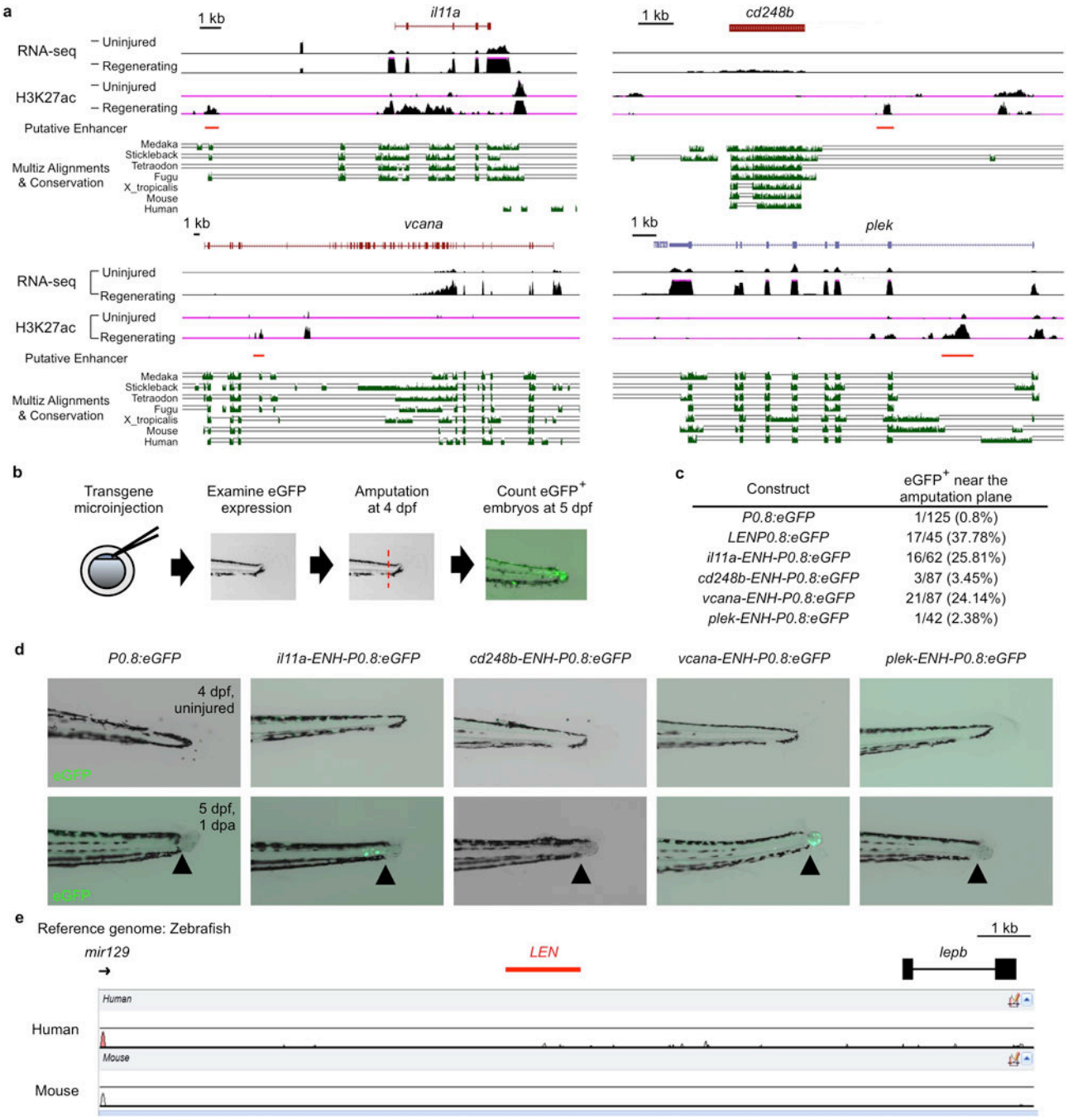

Extended Data Figure 4. Additional putative regeneration enhancer elements

a, Cartoon depicting the distal upstream regions of *il11a, cd248b, vcana*, and *plek.* RNA-sequencing profiles indicate that these genes are upregulated during heart regeneration. The red bar indicates putative enhancer regions that are enriched with H3K27ac marks in regenerating tissue. Two of these putative enhancers, near *il11a* and *vcana*, showed primary sequence conservation in other non-mammalian vertebrates but not in mammals. **b**, Scheme depicting assays in injected F_0 transgenic animals. At 4 dpf, eGFP expression in the uninjured fin fold was examined, and then the fin fold was amputated. eGFP expression near

the amputation plane was examined at 5 dpf. **c**, Table indicating injected constructs and the number of animals with eGFP$^+$ cells near the amputation plane. **d**, Images of representative 4 dpf (uninjured) and 5 dpf (regenerating) fin folds from animals in (**c**). **e**, Vista plot of genomic regions from *mir129* to *lepb* based on *LAGAN* alignment with reference sequence zebrafish. Sequence comparison indicates that this region is not highly conserved between zebrafish and mammals. Arrowheads, amputation planes.

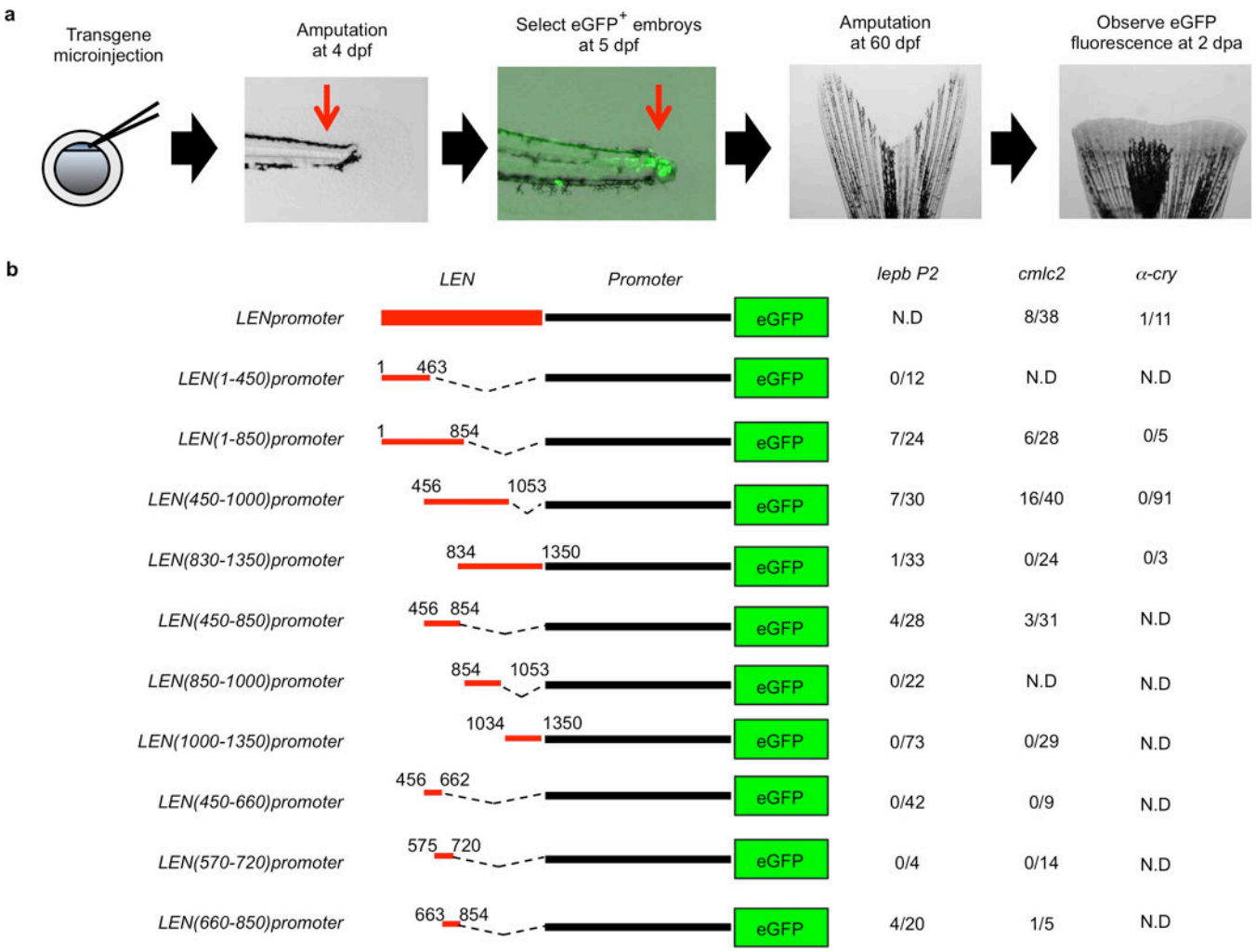

Extended Data Figure 5. Transient transgenic assays examining *lepb*-linked regeneration enhancer fragments in combination with different promoters (fin regeneration)

a, Scheme depicting assays in injected F_0 transgenic animals. Transgene-positive larvae were selected by detection of eGFP in response to fin fold amputation (*lepb* promoter), in cardiomyocytes (*cmlc2* promoter), or in lenses (*α-cry* promoter). Caudal fins of F0 transgenic positive zebrafish were amputated at 60–90 days post-fertilization (dpf), and eGFP expression was examined at 2 dpa. **b**, Schematic representation of the transgenic constructs to examine fin regeneration enhancer activity. Expression during fin regeneration and the number of assessed F_0 animals are indicated. Many embryos transgenic for *LEN(1–850)*, *LEN(450–1000)*, *LEN(450–850)*, and *LEN(660–850)* coupled with the *lepb* or *cmlc2*

promoter showed activity during fin regeneration. One of 11 *LENα-cry:eGFP* animals displayed fin eGFP expression, but *LEN(1–850)α-cry:eGFP* and *LEN(450–1000)α-cry:eGFP* did not drive eGFP expression during fin regeneration, indicating that there may be repressive motifs in the *α-cry* promoter fragment that affect fin regeneration enhancer activity (See also Extended Data Fig. 9). N.D., not determined.

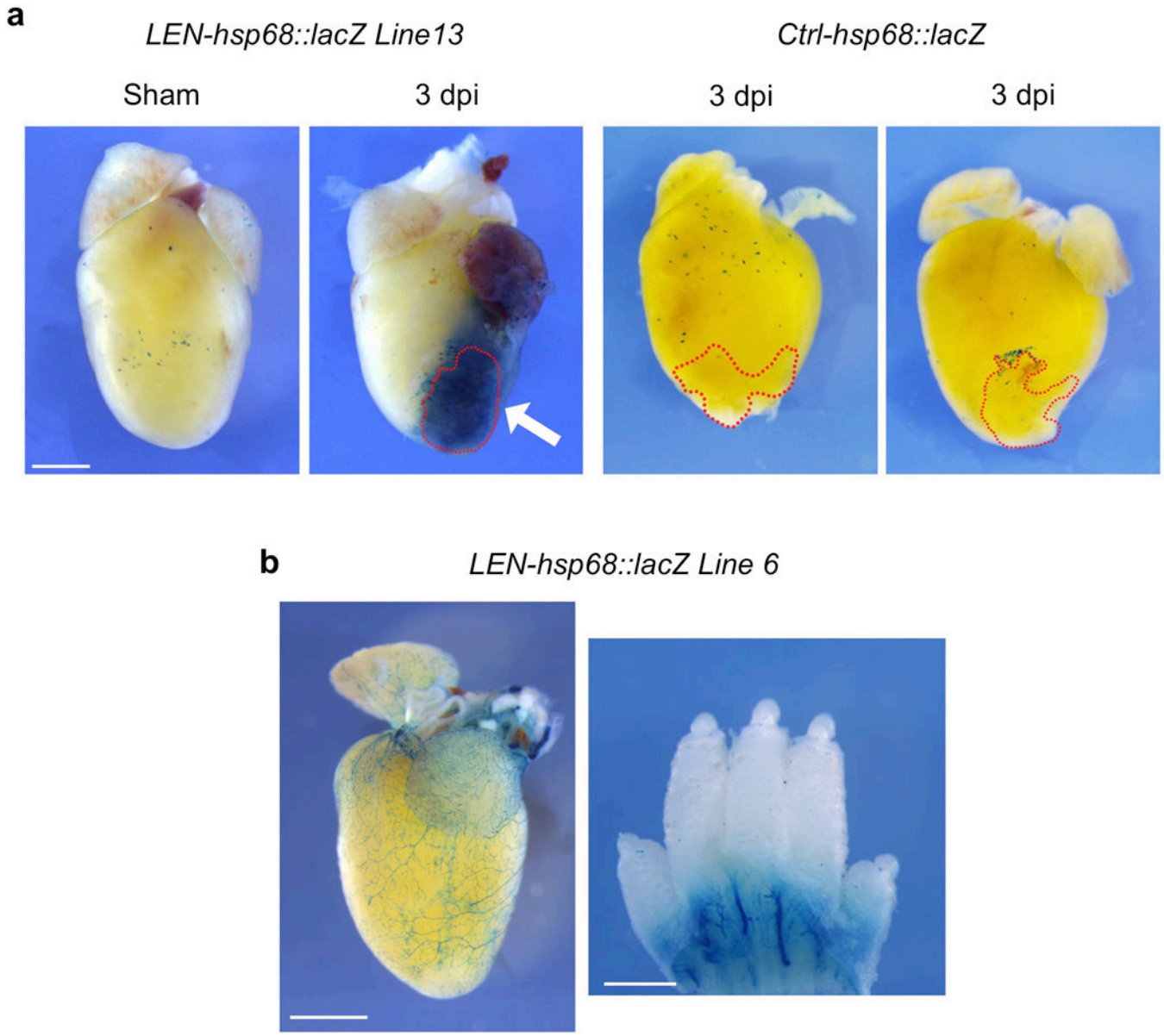

Extended Data Figure 6. X-gal staining in stable transgenic mouse lines

a, Additional whole mount images of X-gal stained hearts from neonatal *LEN-hsp68::lacZ* (line 13, presented in Fig. 3) and control animals injured at postnatal day 1 and assessed at postnatal day 4. X-gal staining is undetectable in sham-operated hearts of *LEN-hsp68::lacZ* mice (n = 6; representative image shown) and injured hearts of control mice, but strong in partially resected hearts of *LEN-hsp68::lacZ* mice (Arrows). Dashed red lines indicate injury

area, positioned facing the front. Arrows, injury-dependent β-galactosidase expression. dpi, days post injury. **b**, Whole mount images of X-gal stained hearts and paws from *LEN-hsp68::lacZ* line 6, which exhibited vascular endothelial expression in uninjured hearts and paws. Scale bars: 1 mm.

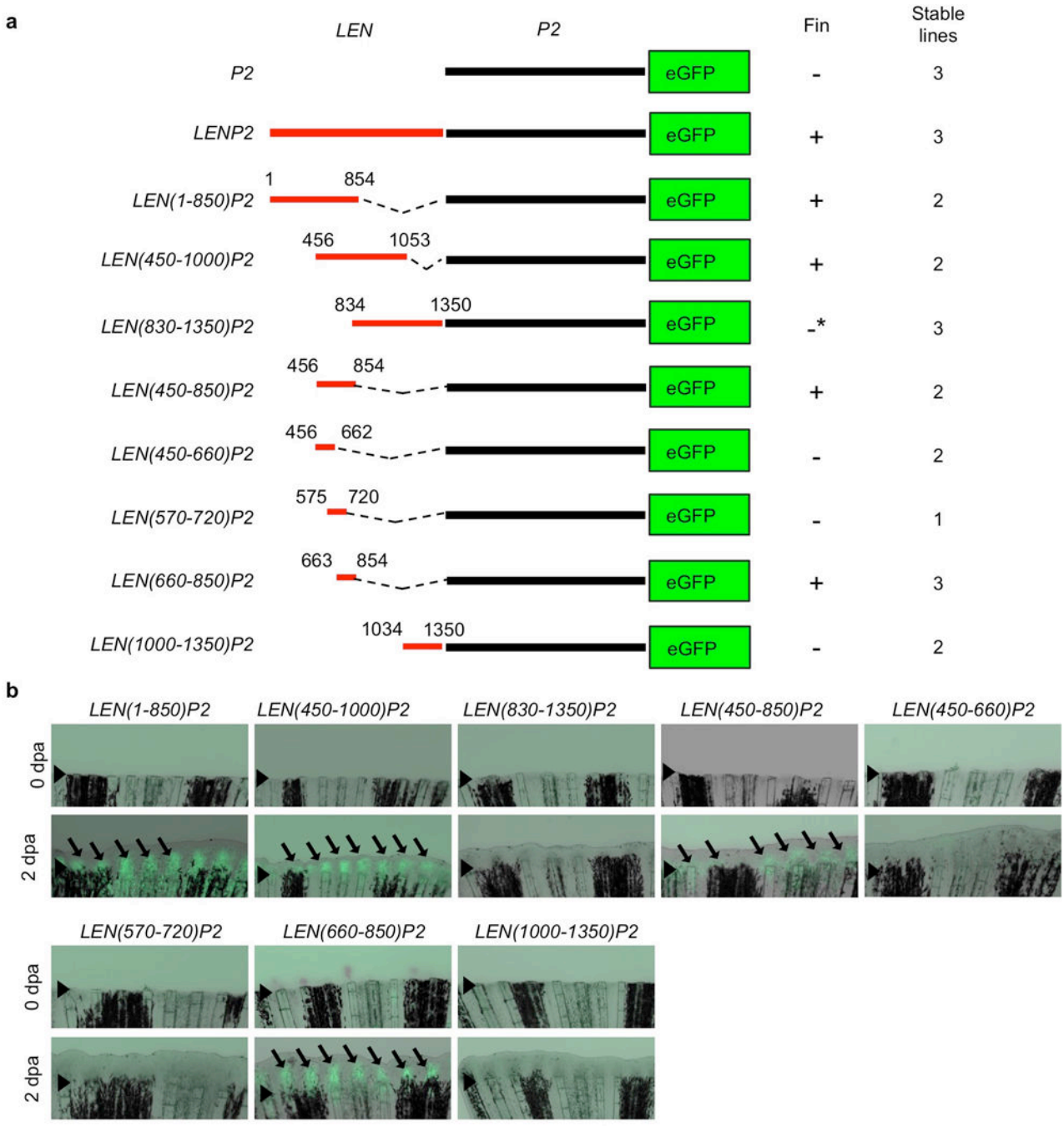

Extended Data Figure 7. Transgenic assays examining *lepb*-linked regeneration enhancer fragments in combination with *lepb P2* (fin regeneration)

a, Schematic representation of the transgenic constructs to examine *LEN* fragments that drive expression during fin regeneration. Expression during fin regeneration and the number

of stable lines is indicated. **b**, Images of representative 0 dpa and 2 dpa fins from **a**. eGFP fluorescence is rarely detectable in uninjured fins. *LEN(1–850)*, *LEN(450–1000)*, *LEN(450–850)*, and *LEN(660–850)* coupled with *P2* drove *eGFP* expression during fin regeneration. **LEN(830–1350)P2:eGFP* lines exhibited very weak eGFP expression in fin regenerates, detectable with long exposure times and at high magnification (data not shown), suggesting the possibility of minor fin regeneration enhancer elements in 850–1000. At least 5 fish from each transgenic line were examined, and all animals displayed a similar expression pattern. Arrowheads, amputation planes.

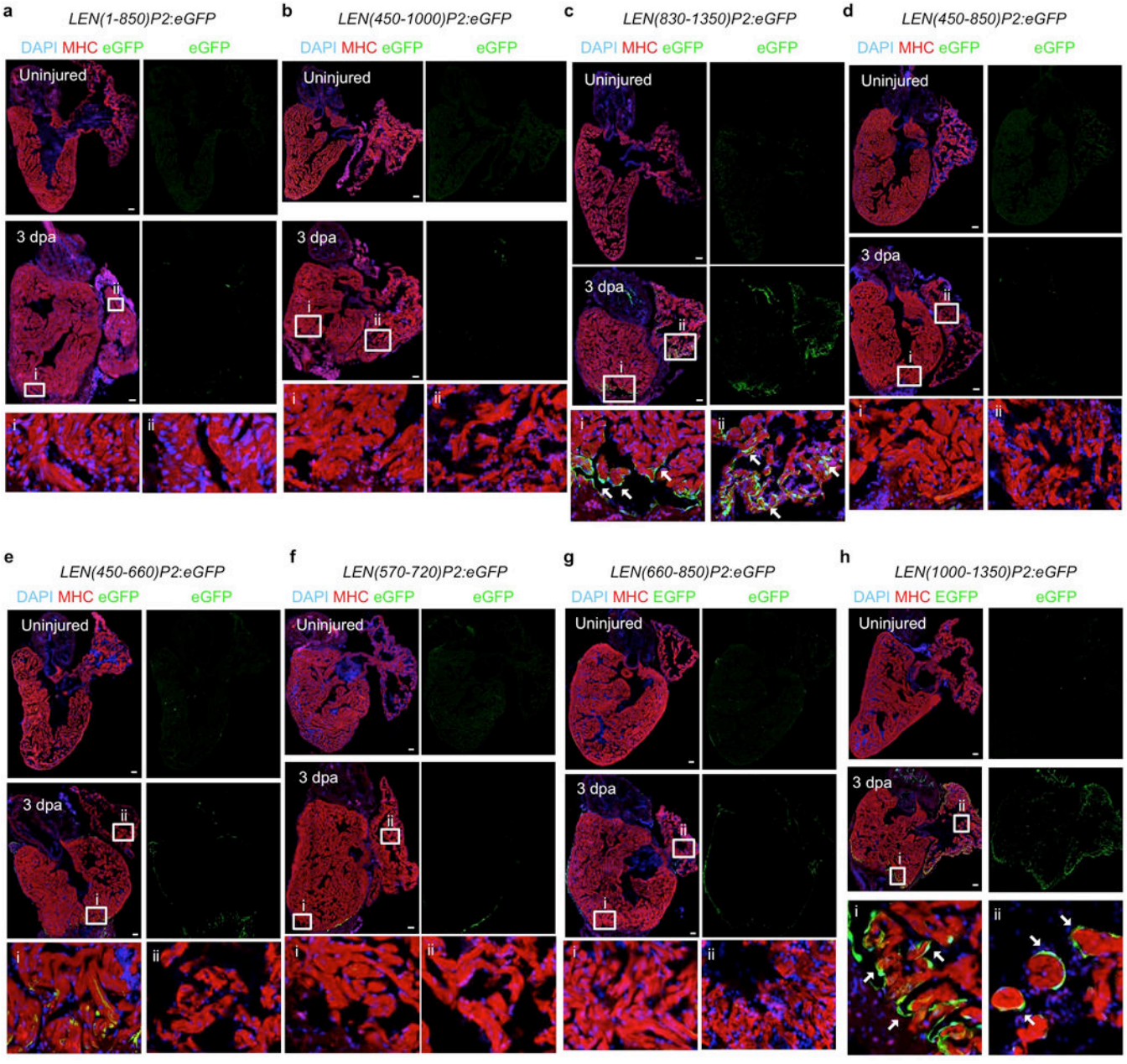

Extended Data Figure 8. Images of heart sections from uninjured and regenerating transgenic lines that employ *lepb*-linked enhancer fragments

a–h, eGFP fluorescence is rarely detectable in uninjured hearts in all transgenic lines. One exception is *LEN(1000–1350)P2:eGFP*, which showed occasional, weak endocardial eGFP expression in uninjured hearts. *LEN(1–850)P2:eGFP* (**a**), *LEN(450–1000)P2:eGFP* (**b**), *LEN(450–850)P2:eGFP* (**d**), and *LEN(660–850)P2:eGFP* (**g)** transgenic lines, which include distal *LEN* elements, directed eGFP expression from promoters in a subset of epicardial cells and/or cardiomyocytes, but not endocardial cells. *LEN(450–660)P2:eGFP* lines (**e**) showed regeneration-dependent enhancer activity in cardiomyocytes near the injury site, but not in endocardial cells. Our data indicated that the activities of *LEN(1–850)P2:eGFP* (**a**), *LEN(450–1000)P2:eGFP* (**b**), and *LEN(450–850)P2:eGFP* (**d**) lines were not as strong as *LEN(450–660)P2:eGFP* (**e**), suggesting that there might be repressive elements for cardiomyocyte expression outside of sequences *450–660. LEN(830–1350)* (**c**) and *LEN(1000–1350)* (**h**), which did not activate expression from promoters during fin regeneration, could direct endocardial expression in both ventricle and atrium during regeneration, similar to the reference reporters *lepb:eGFP* and *LENP2:eGFP.* Arrows in **c**, **h**, endocardial eGFP. i, ii, Enlargements of the boxed areas in regenerating ventricle and atrium, respectively. At least 5 fish from each transgenic line were examined, and all animals displayed a similar expression pattern. Scale bars, 50 μm.

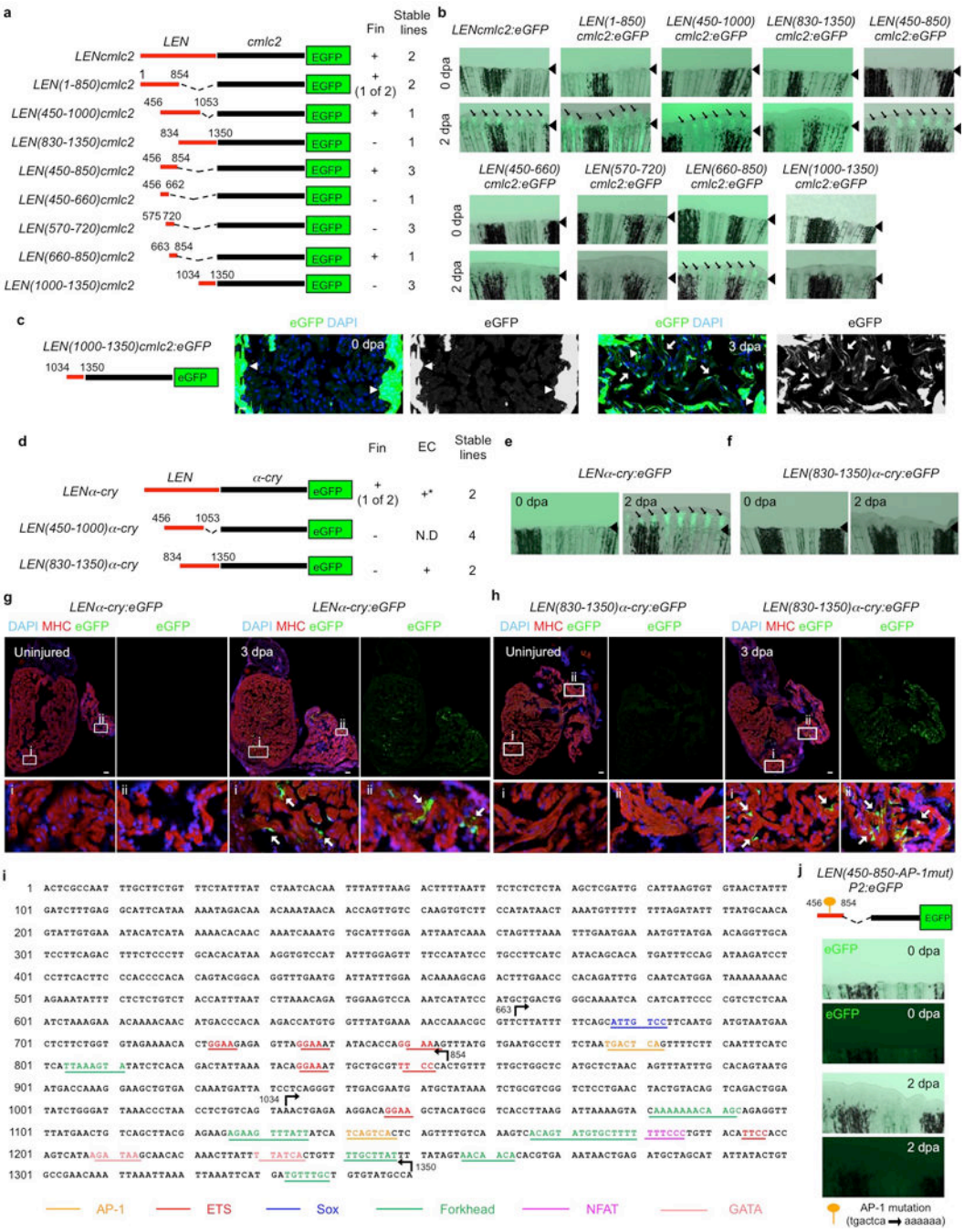

Extended Data Figure 9. Transgenic assays to examine *lepb*-linked enhancer fragment activity in combination with *cmlc2* and *α-cry* promoters

a, Schematic representation of the transgenic constructs to examine enhancer fragment activity in combination with the *cmlc2* promoter. Expression during fin regeneration and the number of stable lines is indicated. **b**, Images of representative 0 dpa and 2 dpa fins from **a**. eGFP fluorescence was very weak or undetectable in 0 dpa or uninjured fins. *(1–850)*, *(450–1000)*, *(450–850)*, and *(660–850) LEN* fragments coupled with the *cmlc2* promoter activated blastemal eGFP fluorescence (arrows) during fin regeneration. One *LEN(1–*

850)cmlc2:eGFP line did not show fin regeneration enhancer activity. Arrowheads, amputation planes. At least five fish from each transgenic line were examined, and all animals displayed a similar expression pattern except for the following: For two strains of *LEN(450–850)cmlc2:eGFP*, 4 of 5 animals induced eGFP fluorescence at 2 dpa; For *LEN(660–850)cmlc2:eGFP*, 4 of 7 animals induced eGFP fluorescence at 2 dpa. **c**, (Left) Schematic diagram of the *LEN(1000–1350)cmlc2:eGFP* transgenic construct. (Right) Images of sections from uninjured and regenerating *LEN(1000–1350)cmlc2:eGFP* hearts. eGFP is expressed mosaically in cardiomyocytes via the *cmlc2* promoter. Uninjured hearts had no detectable endocardial eGFP fluorescence, whereas 3 dpa hearts displayed induced endocardial eGFP fluorescence (arrows). Arrowheads indicate cardiomyocyte eGFP fluorescence driven by *cmlc2* promoter activity. **d–h**, Schematic representation of the transgenic constructs to examine enhancer fragment activity in combination with the *α-cry* promoter. Expression during fin regeneration and injury-activated endocardial expression, and the number of stable lines are indicated. At least 5 fish from each transgenic line were examined, and all animals displayed a similar expression pattern. EC, endocardial cells. One *LENα-cry:eGFP* line showed regeneration-dependent expression (arrows) in fins (**e**); yet, unlike when coupled with *lepb* and *cmlc2* promoters, the *LEN(450–1000)* fragment did not drive expression during fin regeneration (**d** and data not shown). This suggests a possible repressive motif within *α-cry* sequences. *One *LENα-cry:eGFP* line showed weak endocardial eGFP expression in uninjured hearts, but the eGFP signal (arrows) was stronger and broader during regeneration (**g**). Two *LEN(830–1350)α-cry:eGFP* lines had no detectable eGFP fluorescence in regenerating fins (**f**) or uninjured hearts (**h**), but displayed induced endocardial eGFP fluorescence (arrows) during heart regeneration (**h**). i, ii, Enlargements of the boxed areas in regenerating ventricle and atrium, respectively. **i**, *LEN* sequences annotated with putative binding sites in fin- (663–854) and cardiac- (1034–1350) regeneration enhancer modules. **j**, A predicated AP-1 binding site is necessary for fin regeneration enhancer activity. (Top) Schematic representation of the *LEN(450-850-AP-1mut)P2* transgenic construct, in which the predicted AP-1 binding site (tgactca) is mutated to aaaaaa. Two *LEN(450-850-AP-1mut)P2* lines had no detectable eGFP fluorescence in regenerating fins. Scale bars, 50 μm.

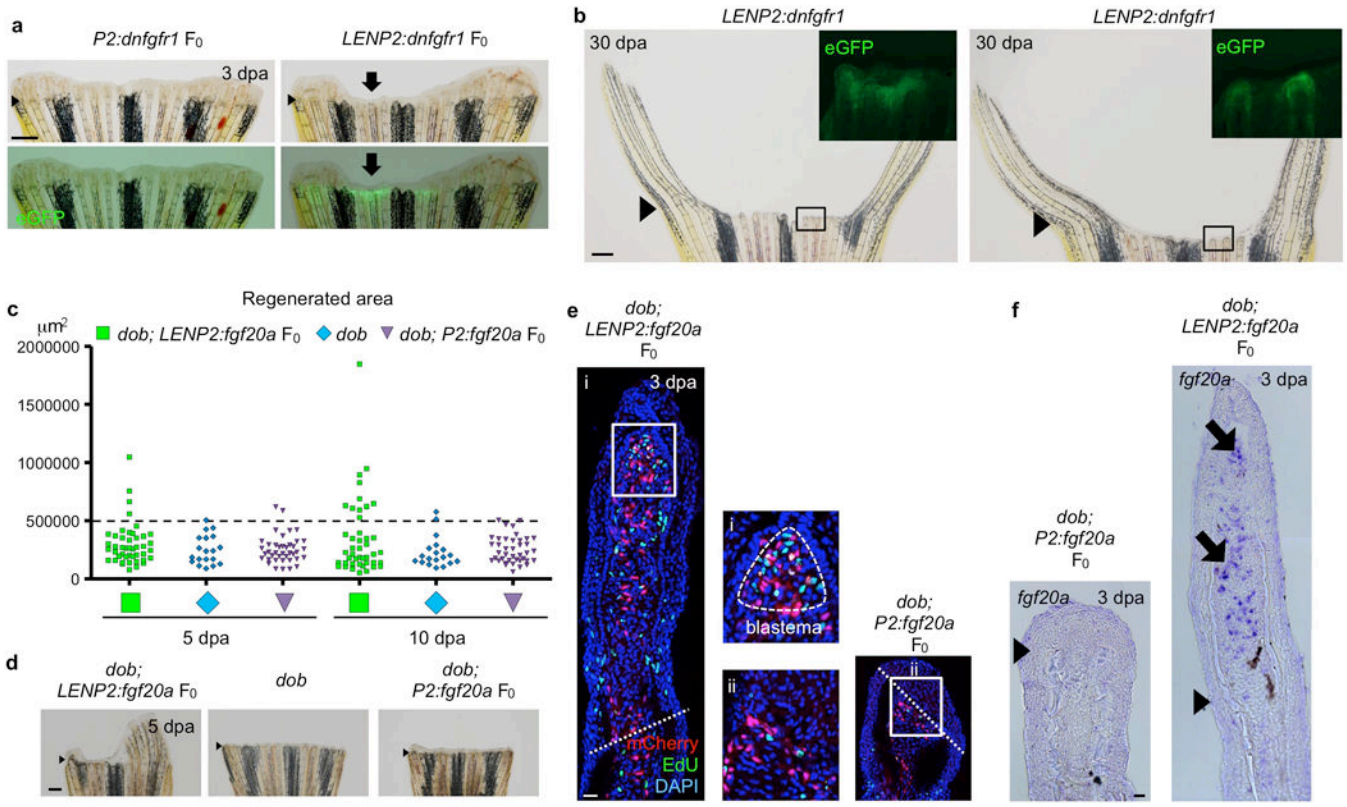

Extended Data Figure 10. Pairing *LEN* with potent developmental influences can control regenerative capacity

a, Images of representative F_0 transgenic zebrafish injected with *P2:dnfgfr1* (left) or *LENP2:dnfgfr1* (right) constructs, shown at 3 dpa. The *dn-fgfr1* cassette is fused in frame to *eGFP*. Whereas zero of 27 *P2:dnfgfr1* F0 animals displayed defective regeneration, 7 of 67 *LENP2:dnfgfr1* F_0 zebrafish had impaired fin regeneration in some fin rays, corresponding to eGFP fluorescence (arrow). **b**, Additional examples of *LENP2:dnfgfr1* fins at 30 dpa, from experiments with a stable line. Inset in **b**, high magnification view of the boxed area, showing eGFP fluorescence. **c**, Quantification of regenerated area from *dob; LENP2:fgf20a* F_0 transgenic zebrafish (n = 45, 44 at 5, 10 dpa), *dob* mutants (n = 19, 19 at 5, 10 dpa), and *dob; P2:fgf20a* F_0 transgenic zebrafish (n = 40, 40 at 5, 10 dpa) at 5 dpa and 10 dpa. Dotted line indicates 500,000 μm^2. **d**, Images of representative *dob; LENP2:fgf20a* F_0 transgenic zebrafish, *dob* mutants, and *dob; P2:fgf20a* F_0 transgenic zebrafish at 5 dpa. **e**, Confocal images of tissue sections of 3 dpa fin regenerates. Mosaic regenerates indicate expression of the linked *ef1α*:nls-mCherry marker construct (red), and EdU incorporation (collected 60 minutes after injection; green). DAPI, blue. F_0 mosaic *dob; LENP2:fgf20a* regenerates show evidence of distal growth and blastemal EdU incorporation. Arrow, blastema. Dotted lines, amputation planes. i, ii, Enlargements of the boxed areas. **f**, *In situ* hybridization in sections of 3 dpa fin regenerates from *dob; P2:fgf20a* (left) and F_0 mosaic *dob; LENP2:fgf20a* (right) animals, indicating *LEN*-induced *fgf20a* expression in mesenchymal cells and regenerative growth. *fgf20a* is rarely detected in *dob; P2:fgf20a* regenerates. Arrowheads, amputation planes.

Supplementary Material

Refer to Web version on PubMed Central for supplementary material.

Acknowledgments

We thank J. Burris, N. Lee, and T. Thoren for zebrafish care; A. Knecht, and J. Savage for technical advice or assistance; and M. Bagnat, C. Chen, F. Conlon, D. Fox, and M. Mokalled for comments on the manuscript. J.H. was supported by an AHA postdoctoral fellowship (12POST11920060), R.K. by an NIH Clinical Investigator Award (K08 HL116485), V.A.T. by an NSF Graduate Research Fellowship (1106401), and J.A.G. by an NIH postdoctoral fellowship (F32 HL120494). This work was supported by NIH grants to B.L.B. (R01 HL089707 and R01 HL064658) and K.D.P. (R01 GM074057 and R01 HL081674), who acknowledges support from HHMI.

References

1. Poss KD. Advances in understanding tissue regenerative capacity and mechanisms in animals. Nat Rev Gen. 2010; 11:710–722.
2. Nacu E, Tanaka EM. Limb regeneration: a new development? Ann Rev Cell Dev Biol. 2011; 27:409–440. [PubMed: 21801016]
3. Kumar A, Godwin JW, Gates PB, Garza-Garcia AA, Brockes JP. Molecular basis for the nerve dependence of limb regeneration in an adult vertebrate. Science. 2007; 318:772–777. [PubMed: 17975060]
4. Whitehead GG, Makino S, Lien CL, Keating M. T fgf20 is essential for initiating zebrafish fin regeneration. Science. 2005; 310:1957–1960. [PubMed: 16373575]
5. Wehner D, Weidinger G. Signaling networks organizing regenerative growth of the zebrafish fin. Trends Genet. 2015; 31:336–343. [PubMed: 25929514]
6. Consortium, E. P. An integrated encyclopedia of DNA elements in the human genome. Nature. 2012; 489:57–74. [PubMed: 22955616]
7. Roadmap Epigenomics, C. et al. Integrative analysis of 111 reference human epigenomes. Nature. 2015; 518:317–330. [PubMed: 25693563]
8. Lagha M, Bothma JP, Levine M. Mechanisms of transcriptional precision in animal development. Trends Genet. 2012; 28:409–416. [PubMed: 22513408]
9. Visel A, Rubin EM, Pennacchio LA. Genomic views of distant-acting enhancers. Nature. 2009; 461:199–205. [PubMed: 19741700]
10. Giorgio E, et al. A large genomic deletion leads to enhancer adoption by the lamin B1 gene: a second path to autosomal dominant adult-onset demyelinating leukodystrophy (ADLD). Hum Mol Genet. 2015; 24:3143–3154. [PubMed: 25701871]
11. Rebeiz M, Pool JE, Kassner VA, Aquadro CF, Carroll SB. Stepwise modification of a modular enhancer underlies adaptation in a Drosophila population. Science. 2009; 326:1663–1667. [PubMed: 20019281]
12. van den Heuvel A, Stadhouders R, Andrieu-Soler C, Grosveld F, Soler E. Long-range gene regulation and novel therapeutic applications. Blood. 2015; 125:1521–1525. [PubMed: 25617428]
13. Indjeian VB, et al. Evolving New Skeletal Traits by cis-Regulatory Changes in Bone Morphogenetic Proteins. Cell. 2016; 164:45–56. [PubMed: 26774823]
14. Lonfat N, Montavon T, Darbellay F, Gitto S, Duboule D. Convergent evolution of complex regulatory landscapes and pleiotropy at Hox loci. Science. 2014; 346:1004–1006. [PubMed: 25414315]
15. Herranz D, et al. A NOTCH1-driven MYC enhancer promotes T cell development, transformation and acute lymphoblastic leukemia. Nat Med. 2014; 20:1130–1137. [PubMed: 25194570]
16. Zhang Y, et al. Positional cloning of the mouse obese gene and its human homologue. Nature. 1994; 372:425–432. [PubMed: 7984236]
17. Fang Y, et al. Translational profiling of cardiomyocytes identifies an early Jak1/Stat3 injury response required for zebrafish heart regeneration. Proc Natl Acad Sci USA. 2013; 110:13416–13421. [PubMed: 23901114]

18. Kikuchi K, et al. Retinoic acid production by endocardium and epicardium is an injury response essential for zebrafish heart regeneration. Dev Cell. 2011; 20:397–404. [PubMed: 21397850]
19. Heintzman ND, et al. Histone modifications at human enhancers reflect global cell-type-specific gene expression. Nature. 2009; 459:108–112. [PubMed: 19295514]
20. Creyghton MP, et al. Histone H3K27ac separates active from poised enhancers and predicts developmental state. Proc Natl Acad Sci USA. 2010; 107:21931–21936. [PubMed: 21106759]
21. Villar D, et al. Enhancer Evolution across 20 Mammalian Species. Cell. 2015; 160:554–566. [PubMed: 25635462]
22. Blow MJ, et al. ChIP-Seq identification of weakly conserved heart enhancers. Nat Genet. 2010; 42:806–810. [PubMed: 20729851]
23. Simkin J, Han M, Yu L, Yan M, Muneoka K. The mouse digit tip: from wound healing to regeneration. Methods Mol Biol. 2013; 1037:419–435. [PubMed: 24029950]
24. Porrello ER, et al. Transient regenerative potential of the neonatal mouse heart. Science. 2011; 331:1078–1080. [PubMed: 21350179]
25. Park C, Kim TM, Malik AB. Transcriptional regulation of endothelial cell and vascular development. Circ Res. 2013; 112:1380–1400. [PubMed: 23661712]
26. De Val S, et al. Combinatorial regulation of endothelial gene expression by ets and forkhead transcription factors. Cell. 2008; 135:1053–1064. [PubMed: 19070576]
27. Lee Y, Grill S, Sanchez A, Murphy-Ryan M, Poss KD. Fgf signaling instructs position-dependent growth rate during zebrafish fin regeneration. Development. 2005; 132:5173–5183. [PubMed: 16251209]
28. Amaya E, Musci TJ, Kirschner MW. Expression of a dominant negative mutant of the FGF receptor disrupts mesoderm formation in Xenopus embryos. Cell. 1991; 66:257–270. [PubMed: 1649700]
29. Kikuchi K, et al. Primary contribution to zebrafish heart regeneration by gata4(+) cardiomyocytes. Nature. 2010; 464:601–605. [PubMed: 20336144]
30. Polizzotti BD, et al. Neuregulin stimulation of cardiomyocyte regeneration in mice and human myocardium reveals a therapeutic window. Sci Translat Med. 2015; 7:281ra245.
31. Gemberling M, Karra R, Dickson AL, Poss KD. Nrg1 is an injury-induced cardiomyocyte mitogen for the endogenous heart regeneration program in zebrafish. eLife. 2015; 4
32. Bersell K, Arab S, Haring B, Kuhn B. Neuregulin1/ErbB4 signaling induces cardiomyocyte proliferation and repair of heart injury. Cell. 2009; 138:257–270. [PubMed: 19632177]
33. Guenther CA, et al. A distinct regulatory region of the Bmp5 locus activates gene expression following adult bone fracture or soft tissue injury. Bone. 2015; 77:31–41. [PubMed: 25886903]
34. Huang GN, et al. C/EBP transcription factors mediate epicardial activation during heart development and injury. Science. 2012; 338:1599–1603. [PubMed: 23160954]
35. Gemberling M, Bailey TJ, Hyde DR, Poss KD. The zebrafish as a model for complex tissue regeneration. Trends Genet. 2013; 29:611–620. [PubMed: 23927865]
36. Deng W, et al. Reactivation of developmentally silenced globin genes by forced chromatin looping. Cell. 2014; 158:849–860. [PubMed: 25126789]
37. Nawa H, Sotoyama H, Iwakura Y, Takei N, Namba H. Neuropathologic implication of peripheral neuregulin-1 and EGF signals in dopaminergic dysfunction and behavioral deficits relevant to schizophrenia: their target cells and time window. Biomed Res Int. 2014; 697935
38. Montero JC, et al. Neuregulins and cancer. Clin Cancer Res. 2008; 14:3237–3241. [PubMed: 18519747]
39. Poss KD, Wilson LG, Keating MT. Heart regeneration in zebrafish. Science. 2002; 298:2188–2190. [PubMed: 12481136]
40. Wang J, et al. The regenerative capacity of zebrafish reverses cardiac failure caused by genetic cardiomyocyte depletion. Development. 2011; 138:3421–3430. [PubMed: 21752928]
41. Suster ML, Abe G, Schouw A, Kawakami K. Transposon-mediated BAC transgenesis in zebrafish. Nat Protocols. 2011; 6:1998–2021. [PubMed: 22134125]
42. Burns CG, et al. High-throughput assay for small molecules that modulate zebrafish embryonic heart rate. Nat Chem Biol. 2005; 1:263–264. [PubMed: 16408054]

43. Kurita R, et al. Suppression of lens growth by alphaA-crystallin promoter-driven expression of diphtheria toxin results in disruption of retinal cell organization in zebrafish. Dev Biol. 2003; 255:113–127. [PubMed: 12618137]
44. Dodou E, Xu SM, Black B. L mef2c is activated directly by myogenic basic helix-loop-helix proteins during skeletal muscle development in vivo. Mech Dev. 2003; 120:1021–1032. [PubMed: 14550531]
45. Kothary R, et al. Inducible expression of an hsp68-lacZ hybrid gene in transgenic mice. Development. 1989; 105:707–714. [PubMed: 2557196]
46. Mahmoud AI, Porrello ER, Kimura W, Olson EN, Sadek HA. Surgical models for cardiac regeneration in neonatal mice. Nat Protocols. 2014; 9:305–311. [PubMed: 24434799]
47. Trapnell C, Pachter L, Salzberg SL. TopHat: discovering splice junctions with RNA-Seq. Bioinformatics. 2009; 25:1105–1111. [PubMed: 19289445]
48. Robinson MD, McCarthy DJ, Smyth GK. edgeR: a Bioconductor package for differential expression analysis of digital gene expression data. Bioinformatics. 2010; 26:139–140. [PubMed: 19910308]
49. Bowman SK, et al. Multiplexed Illumina sequencing libraries from picogram quantities of DNA. BMC Genom. 2013; 14:466.
50. Langmead B, Salzberg SL. Fast gapped-read alignment with Bowtie 2. Nat Meth. 2012; 9:357–359.
51. Zhang Y, et al. Model-based analysis of ChIP-Seq (MACS). Gen Biol. 2008; 9:R137.
52. Lee Y, et al. Maintenance of blastemal proliferation by functionally diverse epidermis in regenerating zebrafish fins. Dev Biol. 2009; 331:270–280. [PubMed: 19445916]
53. Salic A, Mitchison TJ. A chemical method for fast and sensitive detection of DNA synthesis in vivo. Proc Natl Acad Sci USA. 2008; 105:2415–2420. [PubMed: 18272492]

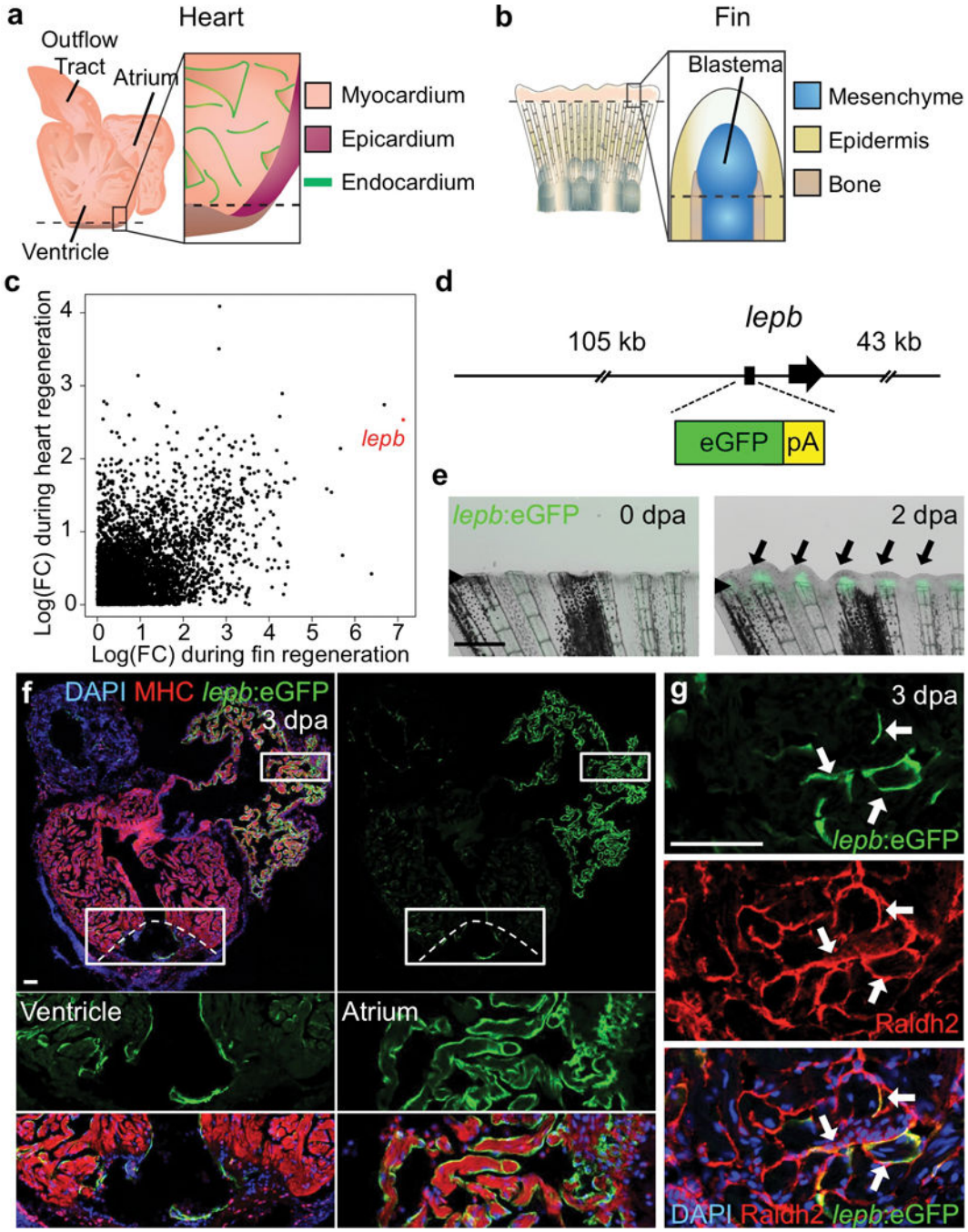

Figure 1. Activation of *lepb* regulatory sequences during tissue regeneration

a, b, Regenerating heart (**a**) and fin (**b**) tissues. **c**, Genes with increased transcript levels in regenerating fins and/or hearts. *lepb* is in red. FC, fold-change. **d**, *lepb:eGFP* BAC transgenic construct, with the first exon replaced by *eGFP*. **e**, *lepb*:eGFP fluorescence (arrows) is detected in fins regenerating after amputation. dpa: days post-amputation. **f, g**, *lepb*:eGFP fluorescence is undetectable in uninjured hearts (see Extended Data Fig. 1), but induced in regenerating hearts by 3 dpa. *lepb*:eGFP fluorescence (arrows in **g**) does not co-localize with MHC^{+} cardiomyocytes (**f**), but co-localizes with $Raldh2^{+}$ endocardial cells (**g**).

Antibodies detected eGFP, MHC, and Raldh2 in **f, g**. n = 8; all animals displayed a similar expression pattern. Scale bars: **e**, 500 μm; **f, g**, 50 μm.

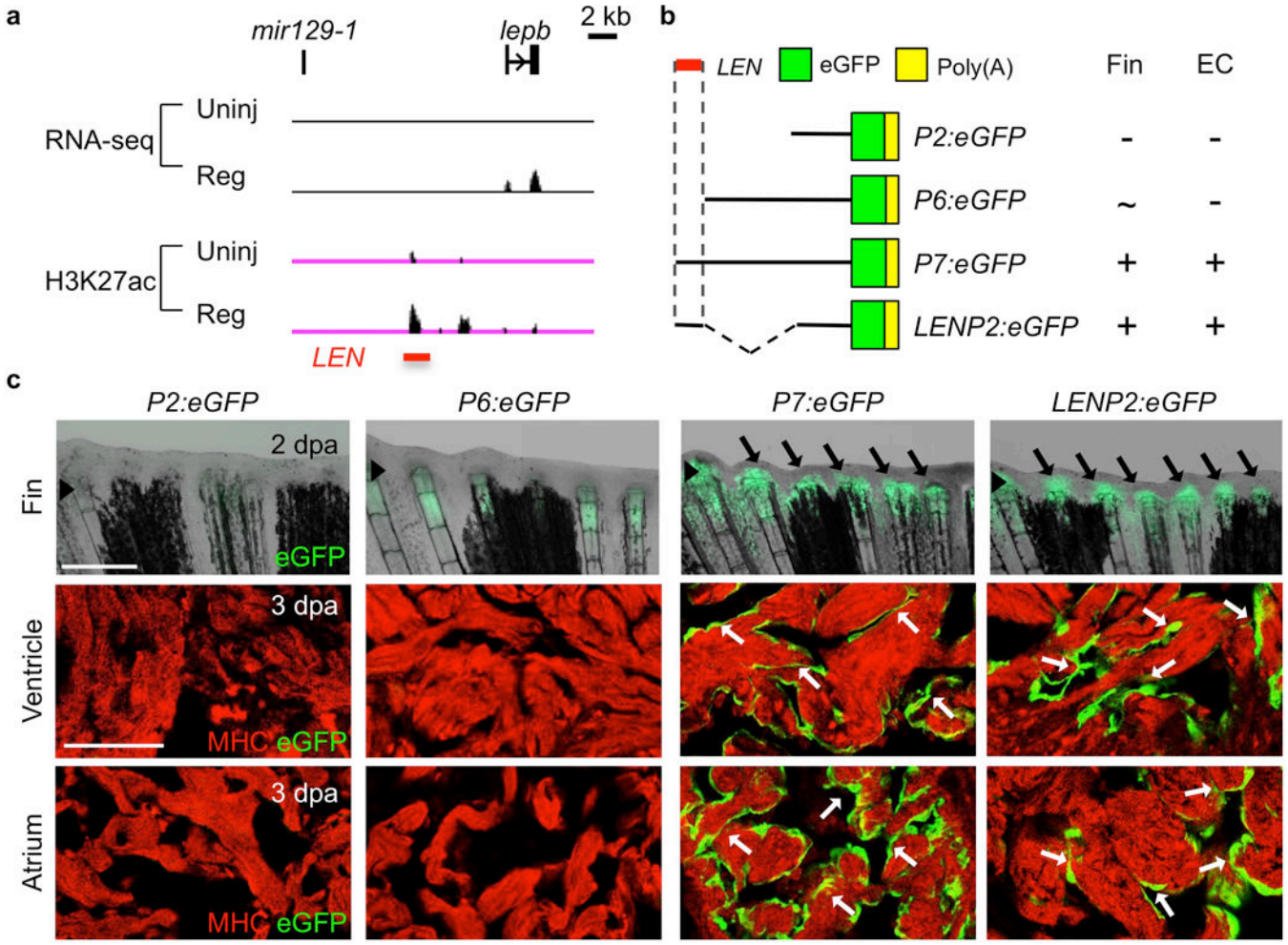

Figure 2. A DNA element upstream of *lepb* directs regeneration-dependent gene expression

a, Genomic DNA regions surrounding *lepb*, indicating RNA-seq and H3K27ac profiles from uninjured and regenerating hearts. Red bar, distal *lepb*-linked element enriched with H3K27ac marks (*LEN*). **b**, Transgene constructs examined for regeneration-dependent expression in fin or heart. EC, endocardial cells. **c**, (Top) Images of 2 dpa regenerating fins from transgenic reporter lines. Arrowhead, amputation plane. Arrows, blastemal eGFP. (Middle) Section images of resected ventricular region at 3 dpa. (Bottom) Atrial tissue distant from injury site. At least 5 fish from each transgenic line were examined, and all animals displayed a similar expression pattern. Arrows, endocardial eGFP. Scale bars: Top, 500 μm; Middle, 50 μm.

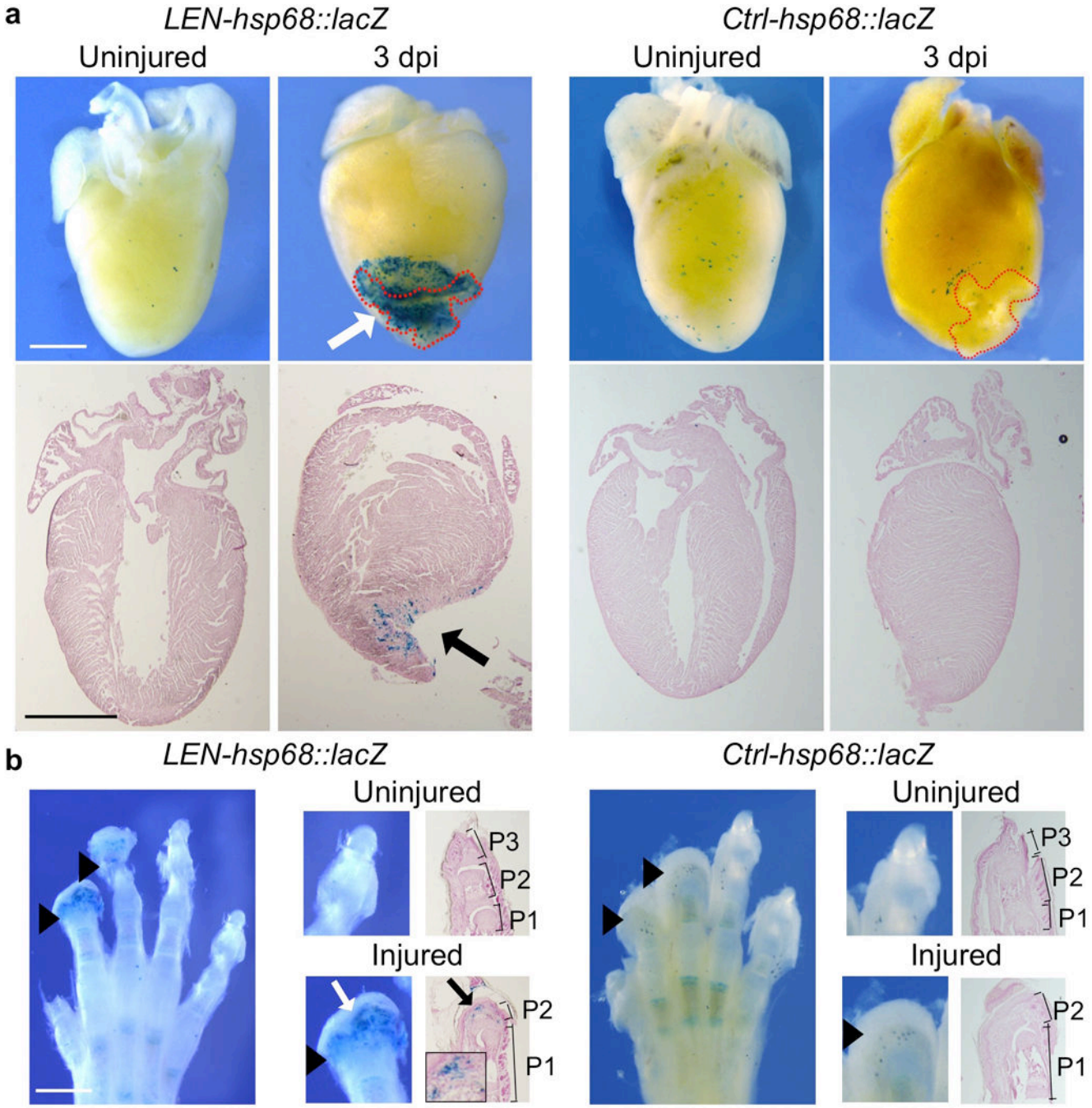

Figure 3. *LEN* activity in neonatal mice

a, Whole-mount (top) and section (bottom) images of X-gal stained hearts of *LEN-hsp68::lacZ* and *Ctrl-hsp68::lacZ* (control) lines, with clear staining in partially resected hearts of *LEN-hsp68::lacZ* mice (arrows) but not controls. n = 5, 5, 6, and 4 for uninjured *LEN-hsp68::lacZ*, 3 days post-injury (dpi) *LEN-hsp68::lacZ*, uninjured control, and 3 dpi control hearts, respectively. Six sham-operated hearts showed minimal staining (see Extended Data Fig. 6). Dashed red lines indicate injury area, positioned facing the front. Arrows, injury-dependent β-galactosidase expression. **b**, Whole-mount (left) and section

(right) images of X-gal-stained digits from these lines, with X-gal staining detectable in amputated, but not uninjured, digits of *LEN-hsp68::lacZ* mice. n = 14(7) and 12(6) for *LEN-hsp68::lacZ* and control digits (animals), respectively. Injuries were performed in neonatal mice on postnatal day 1 and assessed for expression on postnatal day 4. Arrowheads, injury planes. Arrows, injury-dependent β-galactosidase expression. P1, P2, P3, proximal, middle, and distal phalange, respectively. Scale bars: 1 mm.

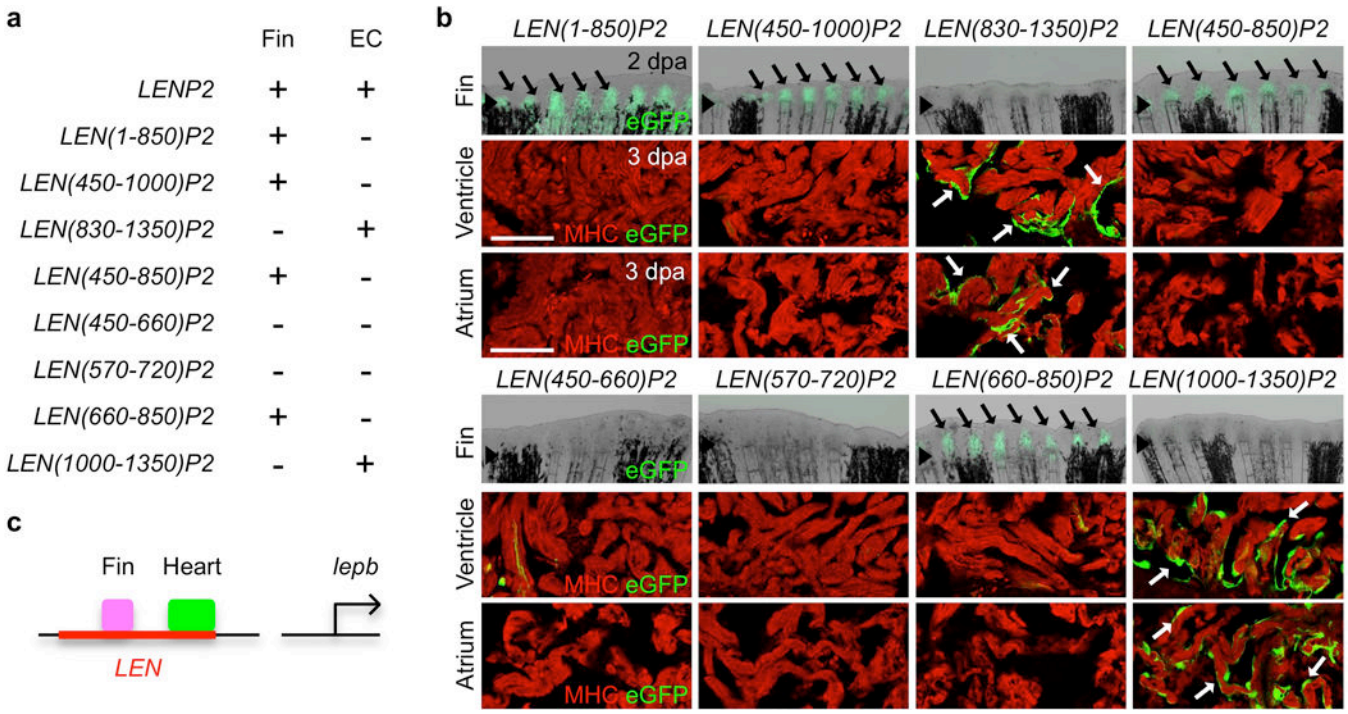

Figure 4. *LEN* is separable into tissue-specific elements

a, Transgene constructs to examine enhancer activation in regenerating fin or cardiac tissue. EC, endocardial cells. **b**, Regenerating fins (top) and sections of cardiac tissue from transgenic lines in **a**. Middle, resected ventricle region. Bottom, atrial tissue distant from injury site. At least 5 fish from each transgenic line were examined, and all animals displayed a similar expression pattern. Arrowheads, amputation plane. Arrows, blastemal (fin) or endocardial (heart) eGFP. **c**, Cartoon indicating separable tissue-specific regeneration modules in *LEN*. Scale bars: **b**, 50 μm.

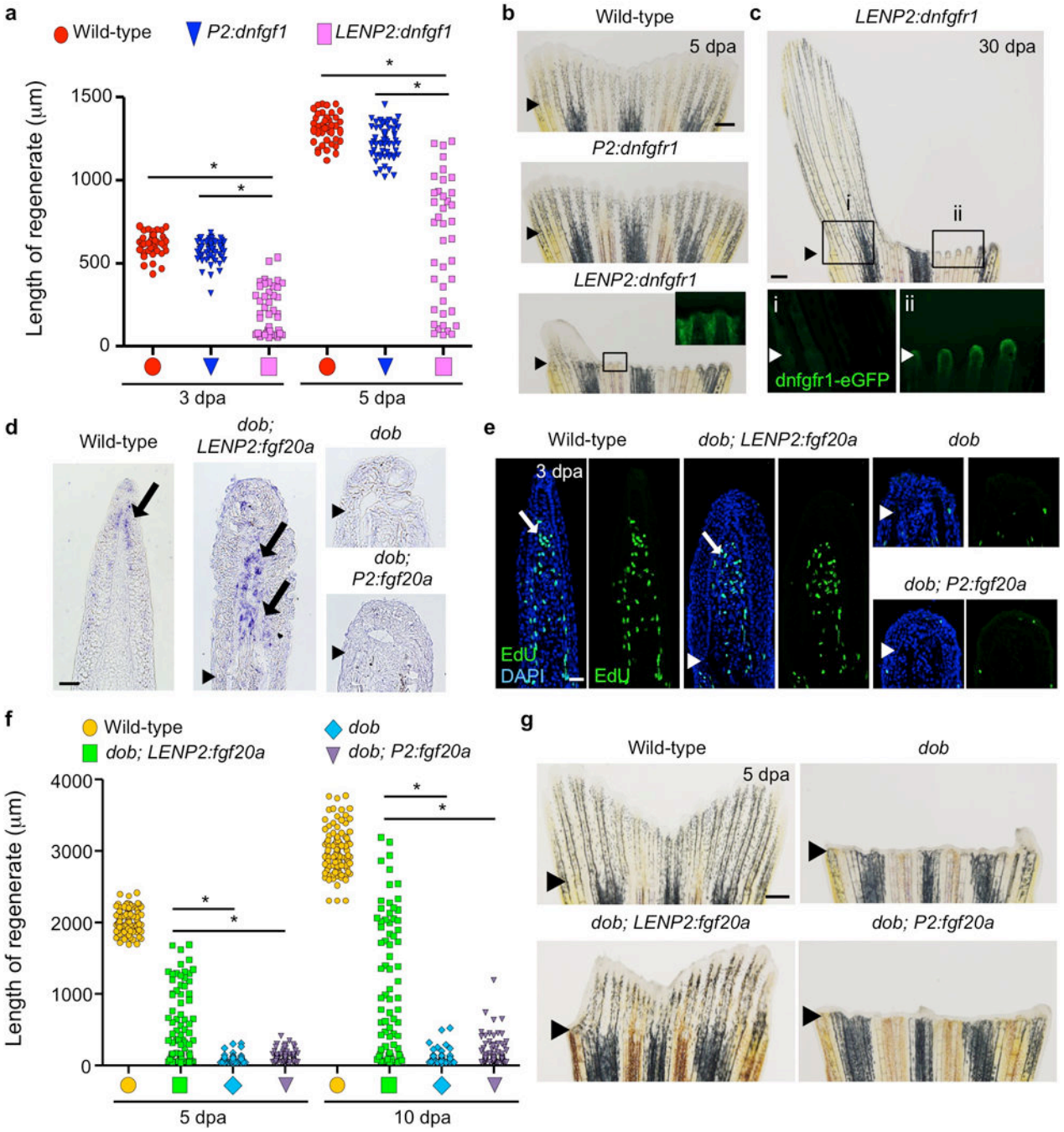

Figure 5. *LEN* controls fin regeneration when paired with Fgf effectors

a, Quantification of 3rd and 4th ray lengths from each lobe at 3 and 5 dpa. *P < 0.01, One-way ANOVA; n = 40 (10), 56 (14), and 40 (10) for wild-type, *P2:dnfgfr1*, and *LENP2:dnfgfr1* fin rays (animals), respectively. **b**, Representative images of 5 dpa fin regenerates that were used for quantification of regenerate lengths in (**a**). Bottom, inset indicates dnfgfr1-eGFP fluorescence from boxed area. **c**, Images of 30 dpa *LENP2:dnfgfr1* fin regenerate. i, ii, eGFP fluorescence from boxed areas, maintained in impaired rays (right). **d**, Section ISH for *fgf20a* expression (arrows) in wild-type, *dob; LENP2:fgf20a*, *dob*,

and *dob; P2:fgf20a* fin regenerates at 3 dpa. **e**, 3 dpa fin regenerates from animals in (**d**), stained for EdU incorporation (green) and nuclei (DAPI, blue), indicating extensive blastemal proliferation in wild-type and *dob; LENP2:fgf20a* regenerates. Fins were collected 60 minutes after EdU injection. **f**, Quantification of 3rd and 4th ray lengths from each lobe at 5 and 10 dpa. *P < 0.01, One-way ANOVA; n = 100 (25), 72 (18), 56 (14), and 100 (25) for wild-type, *dob; LENP2:fgf20a, dob*, and *dob; P2:fgf20a* fin rays (animals) at 5 dpa, respectively; n = 98 (25), 72 (18), 56 (14), and 96 (24) at 10 dpa, respectively. **g**, Representative images of 5 dpa fin regenerates that were used for quantification of regenerate lengths in (**f**). The *LENP2:fgf20a* transgene rescues fin regeneration in *dob* animals, shown with controls at 5 dpa. Arrowheads in **b–e, g**, amputation planes. Scale bars: **b, c, g**, 500 μm; **d, e**, 20 μm.

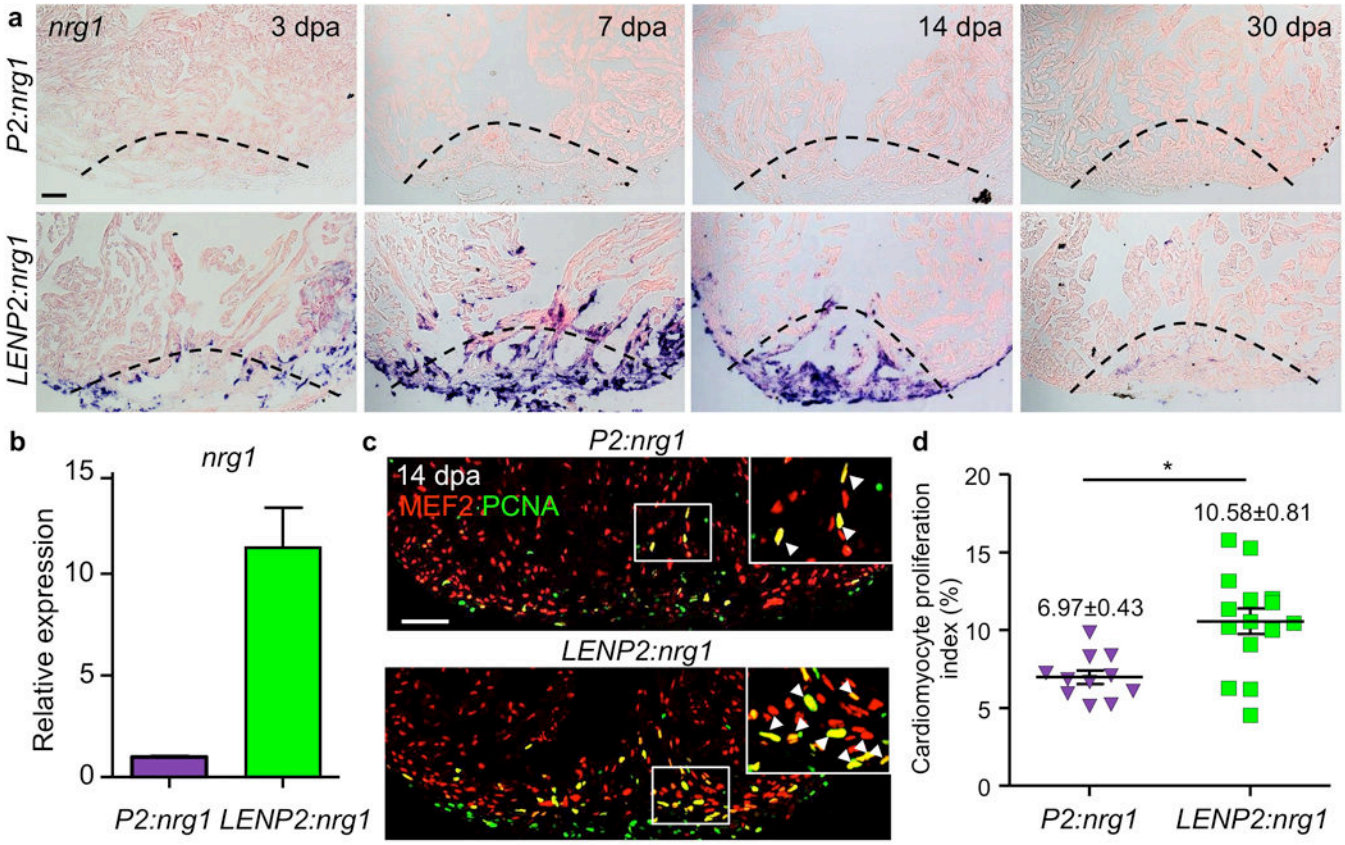

Figure 6. Enhancer-driven *nrg1* expression boosts cardiomyocyte proliferation

a, Representative images of section ISH for *nrg1* in *P2:nrg1* (top) and *LENP2:nrg1* (bottom) ventricles, at several times post-resection. *P2:nrg1:* n = 4, 8, 7, and 3 for 3, 7, 14, and 30 dpa, respectively. *LENP2:nrg1:* n = 4, 8, 8, and 4 for 3, 7, 14, and 30 dpa, respectively. Dashed lines, approximate resection planes. *nrg1* (violet) is sharply induced in endocardial and epicardial cells in *LENP2:nrg1* ventricular injuries. **b**, qPCR analsysis of *nrg1* in whole *P2:nrg1* or *LENP2:nrg1* cardiac ventricles at 3 dpa. **c**, Section images of 14 dpa regenerating ventricular apices from *P2:nrg1* (top) and *LENP2:nrg1* (bottom) animals, stained for cardiomyocyte nuclei (MEF2; red) and the proliferation marker PCNA (green). Insets indicated high-magnification view of regenerating area. Arrowheads, $MEF2^{+}PCNA^{+}$ cardiomyocytes. **d**, Quantified cardiomyocyte proliferation indices in injury sites in experiments from **c**. *P < 0.01, Mann-Whitney rank sum test ; n = 11 (*P2:nrg1*) and 15 (*LENP2:nrg1*). Scale bars: **a, c**, 50 μm. Error bars indicate standard error.